IDENTIFYING OPTIMAL CONCRETE STRENGTH FOR VARYING LEVELS OF BLAST LOADING

Tarek H. Kewaisy
Principal Associate | Louis Berger
1250 23rd St., NW, Washington, DC, 20037, USA

ABSTRACT

This paper reports on the findings of a comprehensive study that involved various numerical simulations of blast-loaded Reinforced Concrete (RC) slabs of different strength classes. The study investigated response characteristics associated with the application of bilinear shock loading of varying intensity and energy levels to one-way RC slabs of various material strengths and boundary conditions. Three strength classes of RC concrete were investigated; Normal Strength (5,000 psi concrete and 60,000 psi rebar), Medium Strength (10,000 psi concrete and 75,000 psi rebar), and High Strength (15,000 psi concrete and 100,000 psi rebar). Nine shock loading profiles were considered by pairing various levels of peak pressure (30 psi for Low, 45 psi for Medium, 60 psi for High) and duration (10 ms for Short, 20 ms for Medium, 40 ms for Long). Two numerical techniques were implemented to simulate strain-rate effects, materials nonlinearities, and damage patterns and extents typically encountered in blast applications: Single Degree Of Freedom- SDOF using RCBlast program and Finite Element Analysis- FEA using LS-DYNA Software. Primary simulation parameters for various RC slab configurations were calibrated using response measurements obtained from testing. The blast testing program was funded by the National Science Foundation (NSF), administered by the University of Missouri – Kansas City (UMKC) and completed at the Blast Loading Simulator (BLS) of the Engineering Research and Development Center (ERDC) at Vicksburg, MS. The effects of considering different strength classes of concrete and reinforcement on the blast response of RC slabs were evaluated. Valuable insights were obtained, and useful conclusions were drawn regarding the appropriateness of use of various material strengths to achieve optimized and enhanced performance of RC slabs subjected to varying levels of blast loading.

INTRODUCTION

In recent years, the design of blast-resistant structures has expanded beyond the boundaries of military and industrial applications into civilian realms including infrastructure, government, public and private buildings. This was primarily driven by the need to protect these assets against the ever growing threat of terrorist attacks using high explosives as the weapon of choice to impart the maximum damage to these prominent targets. The economic impacts of considering such a severe threat combined with the technical engineering challenges to prevent civilian facilities from becoming fortification-like structures have generated strong incentives and considerable motivation among business owners and construction professionals to minimize the impact of blast-resistant design requirements through optimization. Reinforced Concrete (RC) has been the primary construction material for blast hardening for decades, therefore understanding its blast behavior and performance through testing and simulation techniques has been identified as the most important aspect of an optimum blast-resistant design. The accelerated advancements in computing have made numerical simulation techniques (both simplified and advanced) the preferred approaches of: modeling explosives detonation phenomena, identifying blast effects, and

predicting structural behavior to highly-impulsive loads. Due to its economy and time-saving merits, adopting numerical simulation can efficiently provide reliable information about structural responses to various blast loading conditions and hence can be relied upon to guide the optimization process of blast-resistant design of RC structures.

This paper is intended to provide guidance about the optimum selection of RC strength for a specific blast load conditions. The primary structural elements for the study are One-way RC slabs with both simple and fixed support end conditions. Three strength classes of RC concrete incorporating available construction materials were investigated; Normal Strength, Medium Strength and High Strength. Nine bilinear shock loading profiles were considered by pairing various levels of peak pressures (Low, Medium and High) and durations (Short, Medium and Long). These blast profiles were selected to expose the investigated RC slabs to damage levels varying from superficial to severe damage. This was achieved by covering a blast duration to fundamental period ratio (T/T_N) range between 0.50 and 3.50 and a blast intensity to resistance ratio (P/r_u) range between 0.50 and 2.50.

Two numerical techniques were implemented to simulate strain-rate effects, materials nonlinearities, and damage patterns and extents typically encountered in blast applications. 1- Finite Element Analysis- FEA using LS-DYNA Software was primarily utilized to validate the reliability and accuracy of blast predictions produced by various SDOF tools (i.e. RCBlast, UFC 3-340-02 charts and RCProp/ SBEDS) during a previous research work. Primary simulation parameters for various RC slab configurations were calibrated using response measurements obtained from a blast testing program that was funded by the National Science Foundation (NSF) and administered by the University of Missouri – Kansas City (UMKC). 2- Single Degree Of Freedom- SDOF using RCBlast program was adopted as the primary simulation tool for the current study while other SDOF tools were considered for comparison purposes only.

PREVIOUS BLAST SIMULATION WORK USING FEA & SDOF TECHNIQUES

Background Information

Recently, the author participated in a Blast Blind Prediction Contest [7] sponsored by the NSF in collaboration with ACI-447 and ACI-370 committees, Structure-Point and UMKC/ SCE. The contest was successful in drawing the interest of many university academics and practicing engineers who are involved in numerical simulations of RC structural response to blast effects. The main objectives of the contest were to promote technical efforts to improve the accuracy of both analytical SDOF modeling and advanced FEA modeling, to compare the performance of various available simulation tools, and to measure the efficiency of available concrete models implemented in FEA software.

The idea of the contest was initiated by a testing program that was completed at the Blast Loading Simulator (BLS) at the ERDC/ USACE, Vicksburg, MS. The objective of the test program was to investigate the potential advantages of using High Strength Concrete (HSC) with Vanadium Rebar (VR) over Normal Strength Concrete (NSC) with Normal Rebar (NR) for blast-resistant construction. This allowed the collection of a wealth of information about the response of reinforced concrete slabs of various strengths when subjected to various levels of blast loading which was used later in verifying contestants' predictions for different testing configurations.

Test Program Setup

All testing activities took place at the US Army ERDC Center at Vicksburg, MS. RC test specimens were constructed using special wooden forms where concrete was placed over laid rebar. After curing, pressure and strain gauges were attached at designated locations on the face of each specimen. Testing crew used a removable test frame to align each specimen to a test frame fixed into the end wall of the BLS chamber. Once the test specimen was securely attached to the BLS, a shock-like loading was generated inside the BLS tube using either air or helium to achieve the defined blast loading level. Test specimen responses were recorded using high speed video cameras and photography in addition to real-time measurements received from attached gauges.

Figure 1 shows relevant slab geometries and rebar arrangement for tested specimens and their fit within the removable test frame. Figure 2 shows photos of the different stages of a typical test setup.

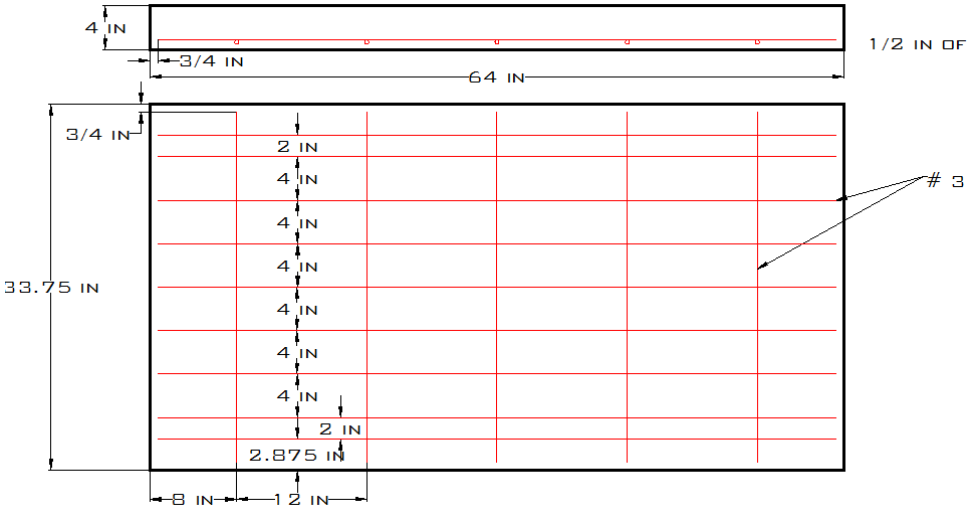

(a) RC Slab Geometry & Rebar Arrangement

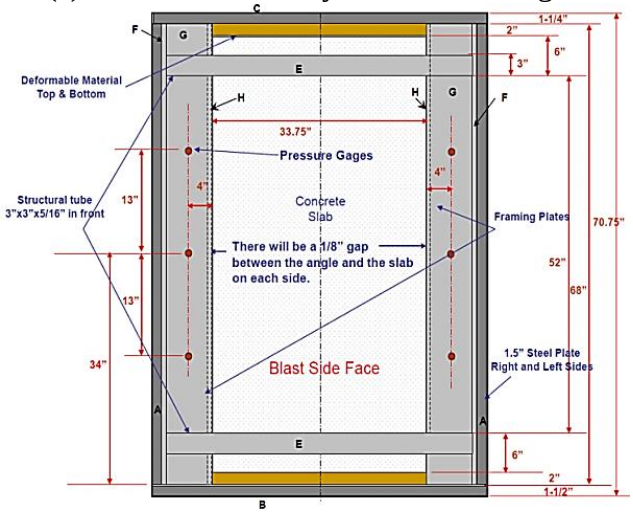

(b) Removable Test Frame

Figure 1- Relevant Test Specimen Information

(a) Preparation

(b) Instrumentation

(c) Attachment

(d) Response Recording

Figure 2- Stages of a Typical Test Setup

Construction Materials

Concrete

Two classes of concrete were considered. Figure 3a shows compressive stress-strain curves constructed using provisions of CEB-FIP 2010 [1] for both NSC: 5400 psi and HSC: 11600psi.

Steel Rebar

Two classes of steel rebar were considered. Figure 3b shows engineering tensile stress-strain curves, approximated using sketches from contest documents [7], for both NR: 72000 psi and VR: 83000 psi.

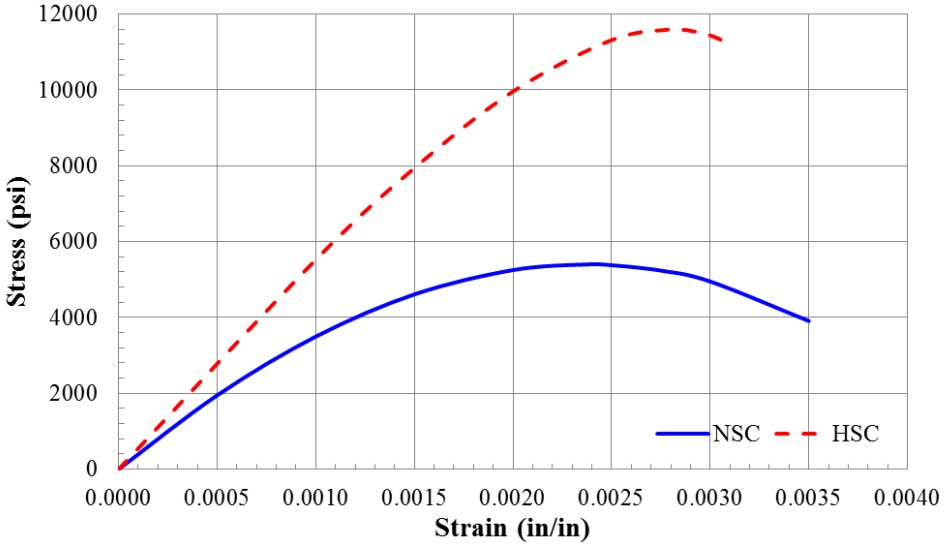

(a) Concrete (Compression)

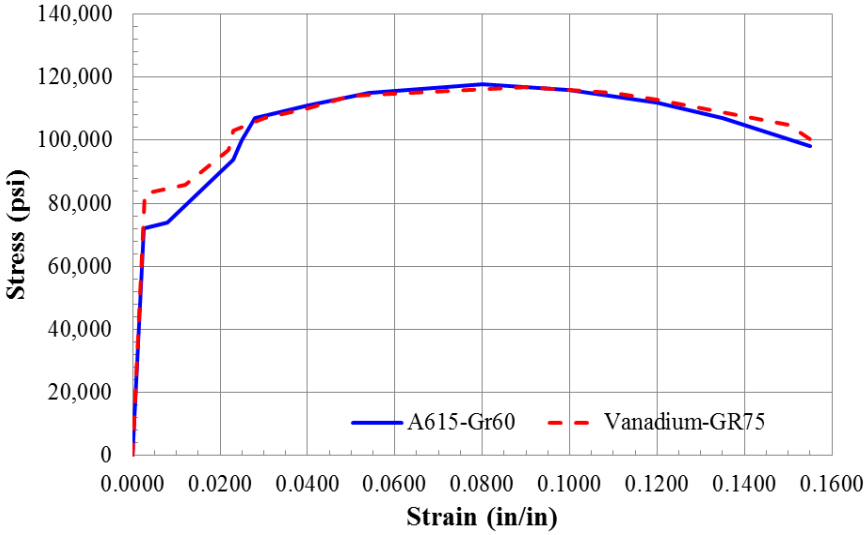

(b) Steel Rebar (Tension)

Figure 3 Stress-Strain Curves for Concrete and Steel Rebar

Blast Loading

A distinct shock load was generated within the BLS for each RC slab configuration and all of which were recorded using direct measurements during testing. Two shock pressure histories were considered for NSCNR slabs namely Set-1a [P_{max} = 50 psi, I_{tot} = 1020 psi.msec], and Set-1b [P = 40 psi, I = 780 psi.msec].

Two shock pressure histories were considered for HSCVR slabs namely Set-2a [P = 49 psi, I = 985 psi.msec], and Set-2b [P = 41 psi, I = 785 psi.msec]. Figure 4 shows shock pressure histories applied to NSCNR and HSCVR slabs.

max

tot

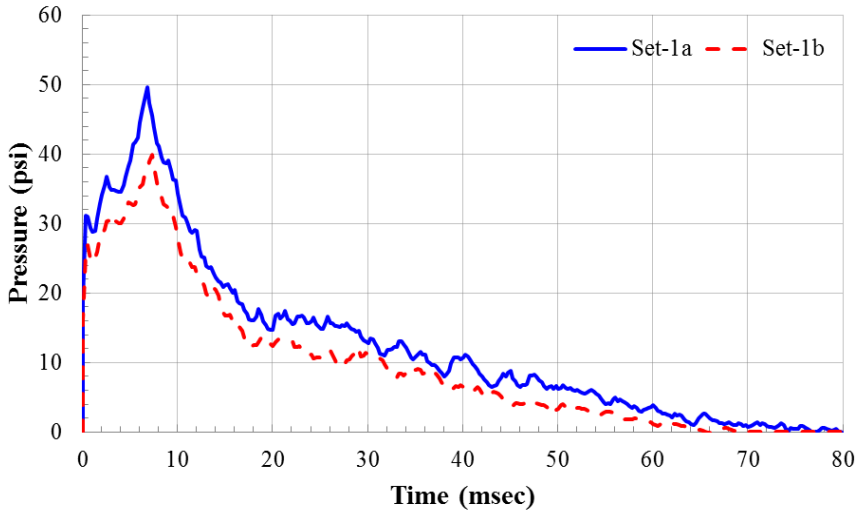

(a) NSCNR Slabs

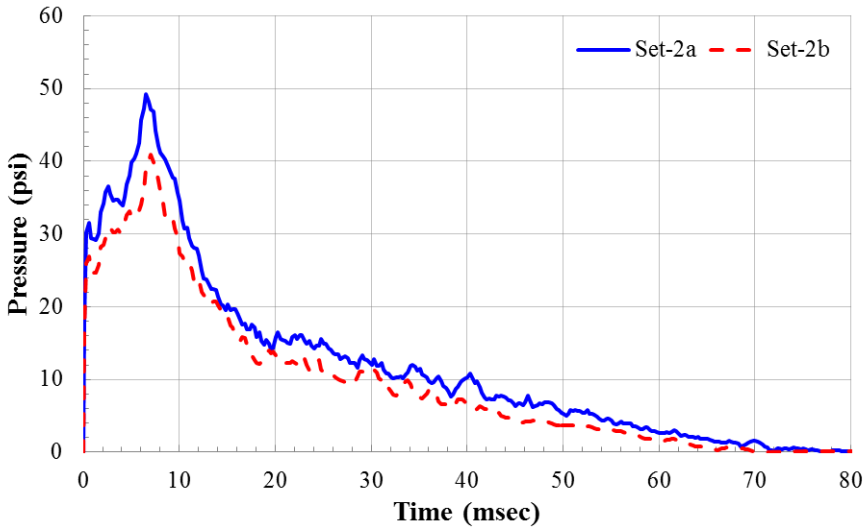

(b) HSCVR Slabs

Figure 4 Shock Pressure Histories

SDOF Simulation

A SDOF model is a simplified mathematical model that represents a dynamic structural/ mechanical system that has an infinite number of Degrees Of Freedom (DOF) using only a single DOF (See Figure 5 below). The determination of the dynamic properties of the equivalent SDOF system is based on the application of principle of conservation of energy. The objective of the SDOF simulation is to compute maximum system responses over time by solving the nonlinear dynamic equilibrium equation representing the system.

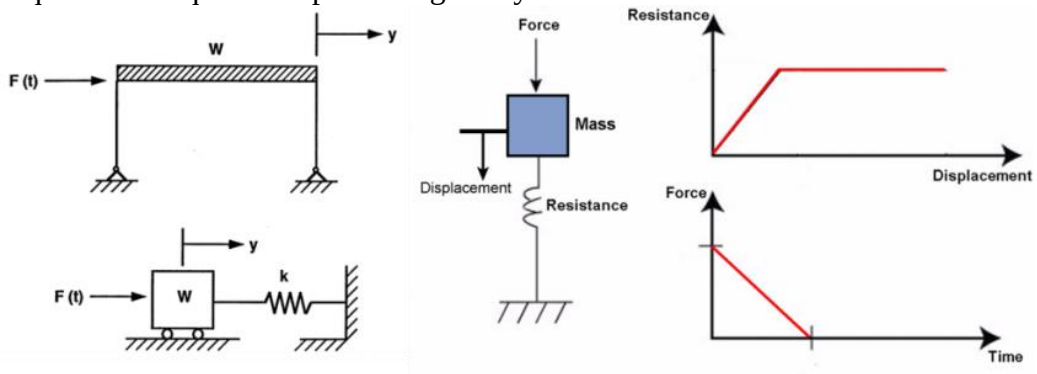

$$M_e\, y''(t) + C_e\, y'(t) + R_e(y(t)) = F_e(t)$$

Where:

M_e	Effective Mass
C_e	Effective Viscous Damping
$R_e(u(t))$	Effective Resistance
$F_e(t)$	Effective Load History
$y''(t)$	Acceleration
$y'(t)$	Velocity
$y(t)$	Displacement

Figure 5- Idealization of A SDOF Model

SDOF Tools

RCBlast [3]

Developed by Eric Jacques, RCBlast is a software for the inelastic dynamic analysis of reinforced concrete structures subject to blast and impact. It allows the user to provide problem-specific information (i.e. geometry, material, boundary conditions, and loading) and it can be used to obtain SDOF displacement history due to a specific dynamic loading or to generate load-independent P-I curves. RCBlast accounts for plastic hinge length and computes moment-curvature profile for the whole response range. RCBlast was selected as the primary SDOF tool for this study due to its unique capabilities of modeling the plastic behavior of concrete elements and its relatively accurate predictions of blast responses.

RCProp/ SBEDS [9]

RCProp is a spreadsheet tool that computes structural properties of RC components using basic principles of force equilibrium and strain compatibility. RCProp utilizes component's geometric parameters, material properties, and boundary conditions to compute equivalent dynamic system parameters required to perform SDOF analyses. SBEDS is an Excel-based tool based on UFC 3-340-02 and can be used for the design and analysis of structural components subjected to dynamic loads using SDOF methodology. For our current application, RCProp is

being used to compute SDOF properties which in turn are used as an input to SBEDS/ General SDOF module to compute SDOF responses to applied blast loading.

UFC-3-340-02 Charts [8]

This Unified Facility Criteria (UFC), is considered to be the primary reference for blast-resistant design by protective design practitioners. Chapter 3 of this resource provides graphical solutions of SDOF elasto-plastic systems subjected to bilinear triangular pulse. For our current investigation, UFC's Figure 3.66 was utilized to estimate primary response parameters; time of maximum response, maximum deflection, and time of initial yield. Only two non-dimensional SDOF ratios are needed to obtain these response estimates namely, load duration to fundamental period ratio and load peak pressure to resistance ratio.

FEA Simulation

Software

LS-DYNA [5], developed by Livermore Software Technology Corporation (LSTC), is a general purpose Hydrocode capable of simulating complex problems especially those involving large deformations, complex boundary conditions, and nonlinear dynamics. This code's is well suited for applications such as automotive crash, explosions and shock wave propagation. It allows the user to select from numerous models representing various material classes including elasticity, plasticity, viscoelasticity, viscoplasticity, composites, thermal effects, and rate dependence. It also provides a large library of elements used to create 3D models including solid, shell, beam, discrete, lumped elements with more than one formulation for each type to suit different applications. To represent various contact conditions, the code supports various algorithms including rigid, flexible, and eroding, linear, surface, edge, and tied contact interfaces.

Geometric Discretization

In (Kewaisy 2016) [4], a partial slab model was considered to reduce the computation time and to allow for finer discretization mesh. The uniform construction of the tested slabs, the use of similar end supports details, and the investigated response type allowed the consideration of symmetry about mid-height and the use of a partial width of the tested slab. Steel rebar was modeled with full integration into the concrete through common nodes with a mesh that has one-element through the rebar section and a one-to-one node along the rebar-concrete interface. Supporting steel tubes were also modeled with a coarse mesh that has one-element through the thickness. A total of 11376 nodes, and 9372 Constant-Strain Solid Elements were used to model the partial concrete slab, interior and exterior supporting steel tubes. Figure 6 below shows an isometric view of the discretized FE model.

Material Models

Three LS-DYNA constitutive models for Concrete and one model for Steel rebar were deemed appropriate for simulating shock response of RC slabs:

> MAT-072-R3 (*MAT_CONCRETE_DAMAGE_REL3) model, developed by Karagozian & Case, is a concrete model based on a three surface plasticity formulation that employs a material damage parameter at each time step to identify a new yield surface for the material. This surface is computed using the three fixed surfaces predefined by the user, and the damage parameter computed at this point. The model requires the use of an Equation Of State (EOS) to describe the pressure-volumetric strain response of concrete.

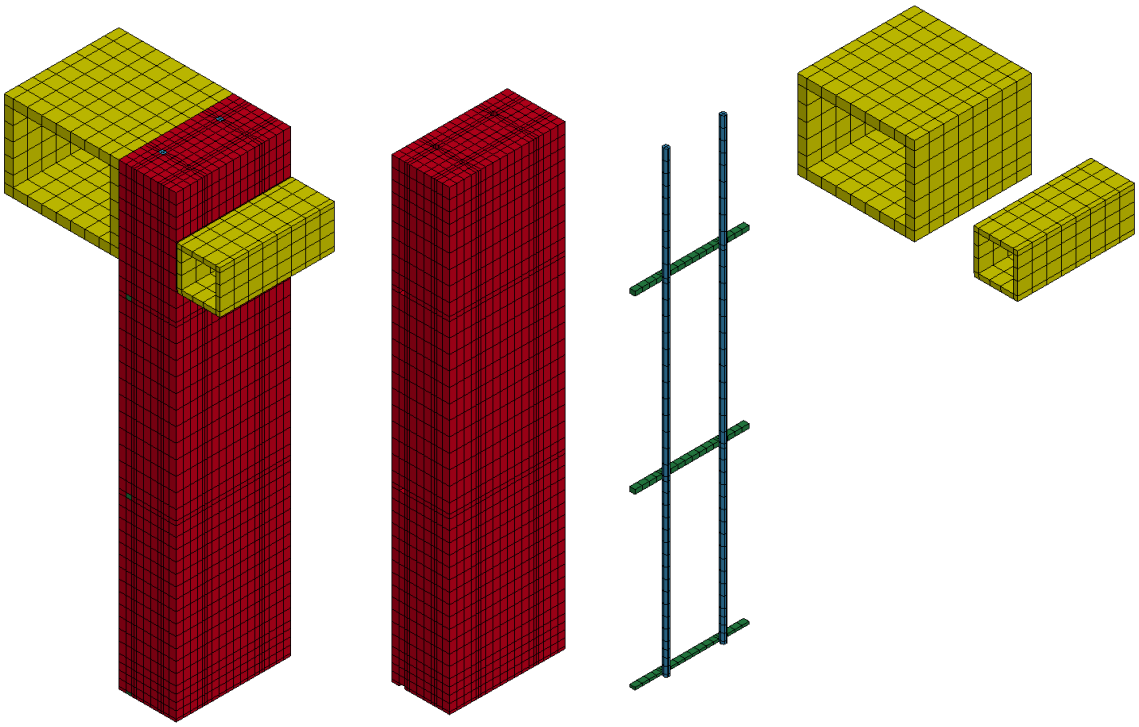

(a) Full Model (b) Concrete (c) Steel Rebar (d) Supporting Tubes

Figure 6 Discretized FE Model for Partial RC Slab and Supports

MAT-072-R3 (*MAT_CONCRETE_DAMAGE_REL3) model, developed by Karagozian & Case, is a concrete model based on a three surface plasticity formulation that employs a material damage parameter at each time step to identify a new yield surface for the material. This surface is computed using the three fixed surfaces predefined by the user, and the damage parameter computed at this point. The model requires the use of an Equation Of State (EOS) to describe the pressure-volumetric strain response of concrete.

MAT-084-085 (*MAT_WINFRITH_CONCRETE) model, developed by Broadhouse B.J. and Nielson, is a smeared crack, smeared rebar model. This model is based upon the four-parameter model in which parameters are functions of the tensile strength to compressive strength ratio and can be determined from uniaxial, biaxail and triaxail compression and tension tests. The model uses radial return which omits material dilation, and includes strain softening in tension expressed in terms of crack opening width or fracture energy.

MAT-159 (*MAT_CSCM_CONCRETE) concrete model, developed by Murray, Y.D., is a cap model with a smooth or continuous intersection between the failure surface and hardening cap. This surface uses a multiplicative formulation to combine the shear (failure) surface with the hardening compaction surface (cap) smoothly and continuously. This type of model is often referred to as a continuous surface cap model (CSCM).

MAT-024 (*MAT_PIECEWISE_LINEAR_PLASTICITY) was selected to represent the nonlinear behavior of both NR and VR steels in addition to the supporting steel tubes. For each steel type, two LOAD CURVES were prepared to capture the material behavior. The first represents the material true- effective stress- effective plastic strain function as computed from original engineering stress-strain curves. The second provides strain-rate vs Dynamic Increase Factor (DIF) as obtained from Malvar and Crawford.

Sample Simulation Results (Kewaisy 2016) [4]

SDOF Predictions

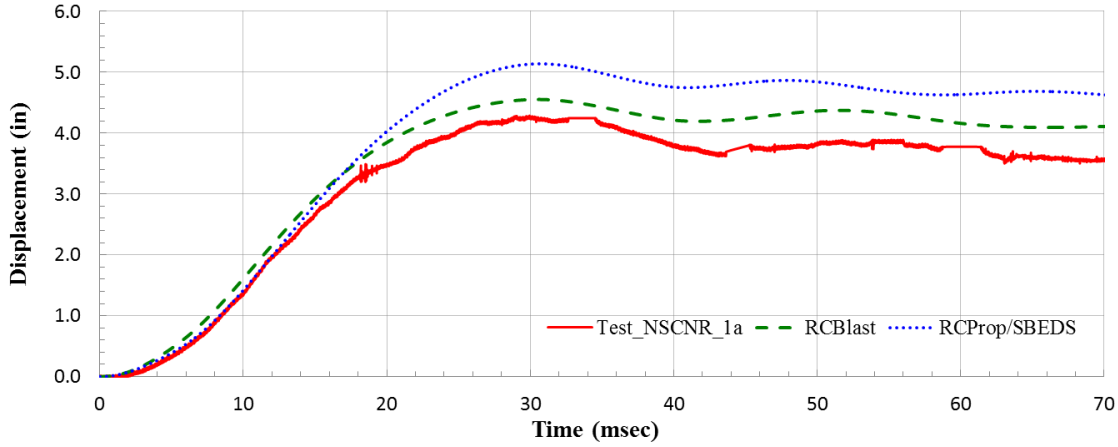

Figure 7 Maximum Displacement Response of NSCNR Slab (SDOF)

Table 1 Summary of SDOF Response Predictions for Normal-Strength Concrete Slab

SDOF TOOL	NSCNR (Set- 1a Blast)					
	Max Displ Y_{max} *in (mm)*	Error Err *%*	Time T_{max} *msec*	Error Err *%*	Resid Displ Y_{res} *in (mm)*	Error Err *%*
TEST	4.287 (108.9)	N/A	29.95	N/A	3.532 (89.7)	N/A
UFC-3-340-02	5.003 (127.1)	16.7%	30.32	1.2%	N/A	N/A
RCBLAST	4.553 (115.7)	6.2%	30.50	1.8%	4.125 (104.8)	16.8%
RCProp/SBEDS	5.140 (130.6)	19.9%	30.67	2.4%	4.585 (116.5)	29.8%

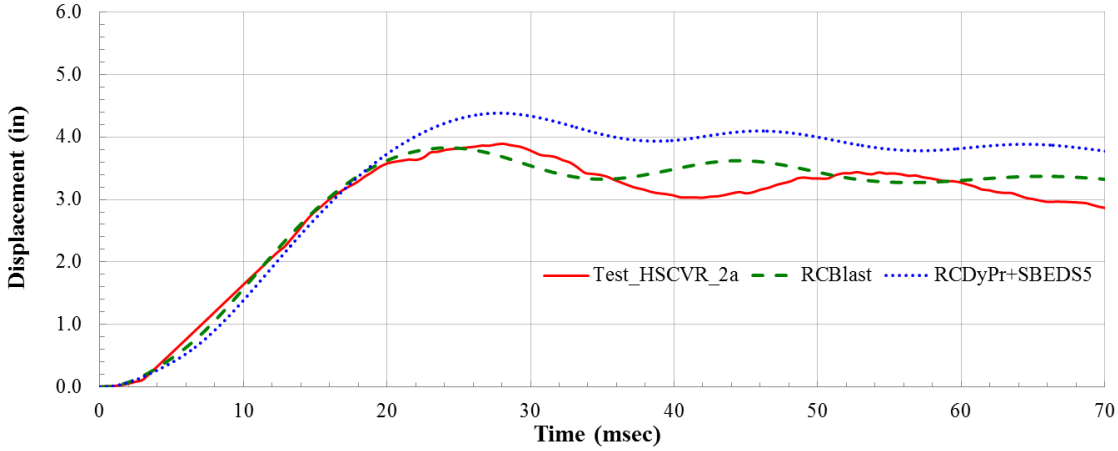

Figure 8 Maximum Displacement Response of HSCVR Slab (SDOF)

Table 2 Summary of SDOF Response Predictions for High-Strength Concrete Slab

SDOF TOOL	HSCVR (Set-2a Blast)					
	Max Displ Y_{max} *in (mm)*	Error Err *%*	Time T_{max} *msec*	Error Err *%*	Resid Displ Y_{res} *in (mm)*	Error Err *%*
TEST	3.890 (98.8)	N/A	28.16	N/A	2.825 (71.8)	N/A
UFC-3-340-02	4.128 (104.9)	6.1%	26.90	-4.5%	N/A	N/A
RCBLAST	3.827 (97.2)	-1.6%	24.20	-14.1%	3.278 (83.3)	16.0%
RCProp/SBEDS	4.382 (111.3)	12.6%	27.80	-1.3%	3.709 (94.2)	31.3%

FEA Predictions

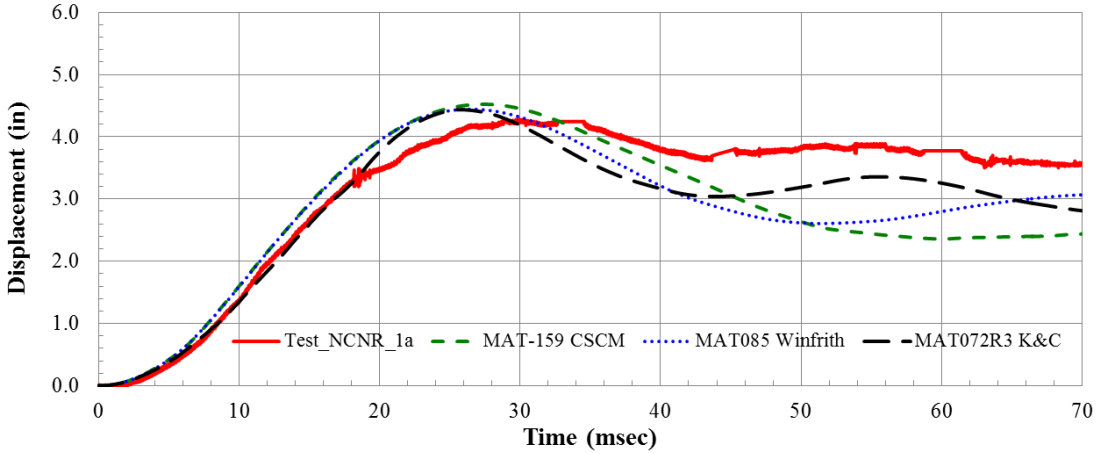

Figure 9 Maximum Displacement Response of NSCNR Slab (FEA)

Table 3 Summary of FEA Response Predictions for Normal-Strength Concrete Slab

LS-DYNA Constitutive Model	NSCNR (Set- 1a Blast)					
	Max Displ Y_{max} *in (mm)*	Error Err *%*	Time T_{max} *msec*	Error Err *%*	Resid Displ Y_{res} *in (mm)*	Error Err *%*
TEST	4.287 (108.9)	N/A	29.95	N/A	3.532 (89.7)	N/A
LS-DYNA MAT-159	4.523 (114.9)	5.5%	27.40	-8.5%	2.450 (62.2)	-30.6%
LS-DYNA MAT-085	4.444 (112.9)	3.7%	26.50	-11.5%	3.076 (78.1)	-12.9%
LS-DYNA MAT-072R3	4.437 (112.7)	3.5%	25.70	-14.2%	2.763 (70.2)	-21.8%

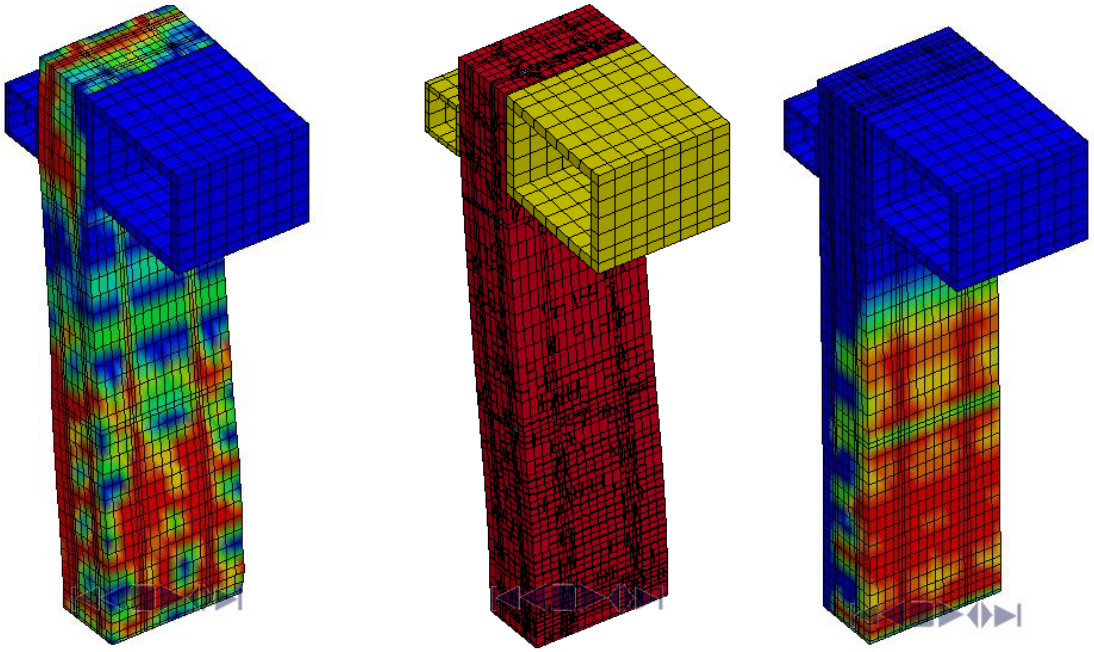

(a) MAT-159 Plastic Strain (b) MAT-084-085 Crack Pattern (c) Mat 072R3 Plastic Strain

Figure 10 NSCNR Slab Cracking Patterns Due to Blast Damage

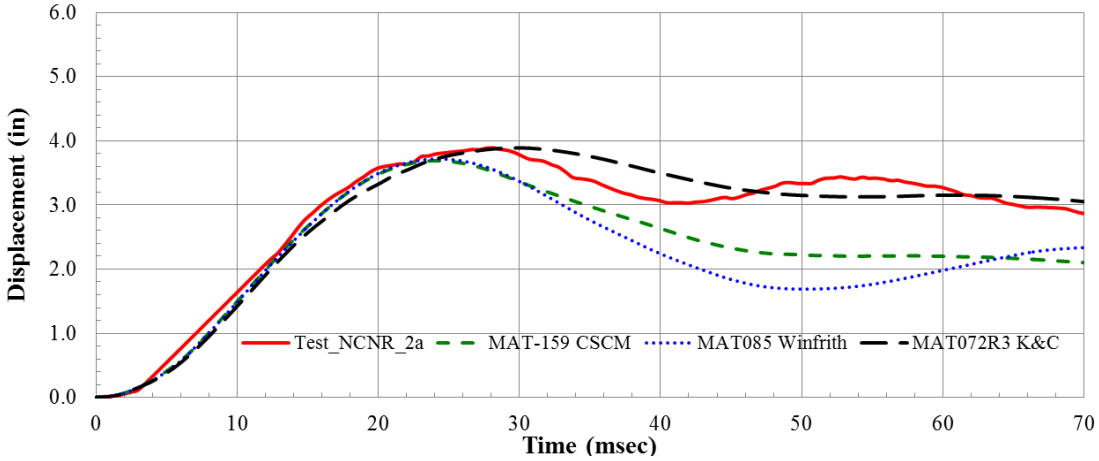

Figure 11 Maximum Displacement Response of HSCVR Slab (FEA)

Table 4 Summary of FEA Response Predictions for High-Strength Concrete Slab

LS-DYNA Constitutive Model	HSCVR (Set-2a Blast)					
	Max Displ Y_{max} *in (mm)*	Error Err *%*	Time T_{max} *msec*	Error Err *%*	Resid Displ Y_{res} *in (mm)*	Error Err *%*
TEST	3.890 (98.8)	N/A	28.16	N/A	2.825 (71.8)	N/A
LS-DYNA MAT-159	3.689 (93.7)	-5.2%	24.10	-14.4%	2.059 (52.3)	-27.1%
LS-DYNA MAT-085	3.716 (94.4)	-4.5%	24.20	-14.1%	2.352 (59.8)	-16.7%
LS-DYNA MAT-072R3	3.888 (98.8)	-0.1%	30.10	6.9%	2.987 (75.9)	5.7%

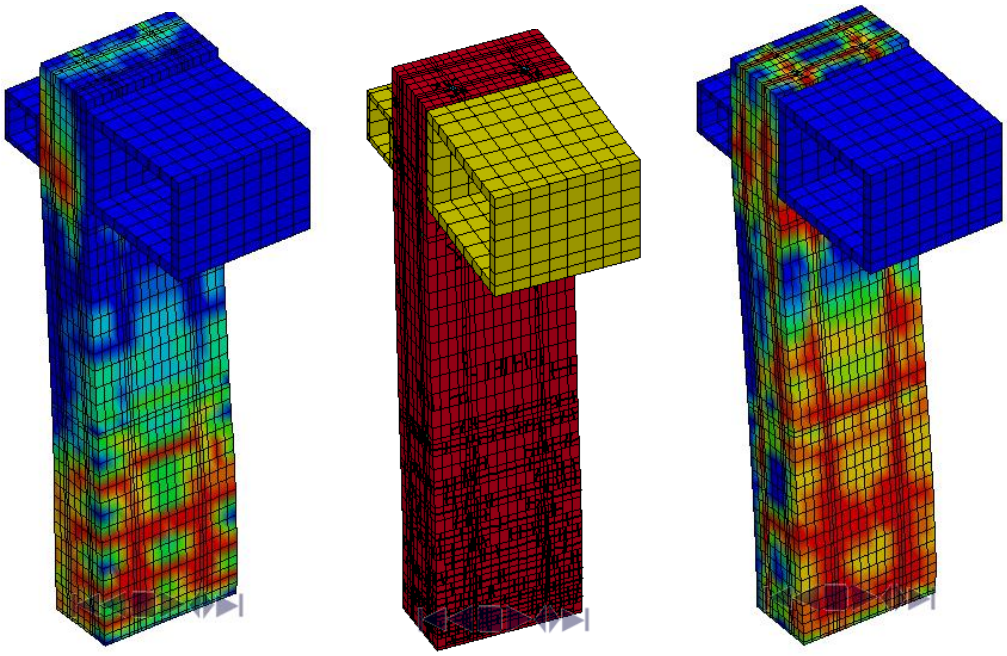

(a) MAT-159 Plastic Strain (b) MAT-084-085 Crack Pattern (c) Mat 072R3 Plastic Strain
Figure 12 HSCVR Slab Cracking Patterns Due to Blast Damage

Conclusions about the Accuracy of Various Simulation Techniques (Kewaisy 2016) [4]

1. Despite their modeling limitations, primary SDOF tools (i.e. RCBlast and RCProp/SBEDS) have exhibited excellent capability of predicting the structural behavior of both NSCNR and HSCVR slabs up to the instant of peak response.
2. As shown in Figures 7, 8 and by inspection of Tables 1, 2, it can be concluded that RCBlast provided better accuracy in its response estimates. With few exceptions, its estimates were within ±10.0% (on average) for maximum displacement and within ±15.0 % (on average) for time of maximum response compared to test measurements. Predictions for residual displacements showed higher levels of deviation and variability with estimates within ±20% (on average) of test measurements.
3. In general, FEA simulations are known to yield accurate predictions compared to those produced by SDOF due to their ability to: accommodate large number of DOF, model realistic non-standard boundary conditions, utilize rigorous material models with nonlinearities, account for varying strain-rate effects, allow for spatially varying shock loading and predict residual damage patterns and extents. Nevertheless, FEA modeling power and precision come at a price as it requires extensive knowledge, expertise, computing power, and modeling time.
4. As shown in Figures 9, 10, 11, 12 and by inspection of Tables 3, 4, it can be concluded that LS-DYNA simulations using various constitutive models, with few exceptions, have provided predictions within ±5.0% (on average) for maximum displacement and within ±10.0 % (on average) for time of maximum response compared to test measurements. Estimates for residual displacements showed higher levels of variability with estimates within ±15% (on average) of test measurements. Deviations from test observations were

primarily attributed to inaccuracies of analytical parameters implemented for various concrete constitutive models.

5. For a certain blast loading, and as observed through test measurements and simulation results, the utilization of a higher strength concrete did not provide a considerable advantage over lower strength concrete in terms of reduced blast response and damage extents.

Based on the findings of the blast prediction study and as per its conclusions, the author identified the need for a comprehensive investigation of the influence of RC materials' strengths on the blast performance of RC concrete slabs. The author made the decision to adopt SDOF techniques for the current investigation acknowledging their acceptable accuracy, ease of use, and manageable computational effort,

INVESTIGATION OF MATERIAL STRENGTH EFFECTS ON BLAST RESPONSE

The current study investigates the factors influencing the appropriate selection of RC strength class for a specific structural configuration and blast loading conditions. The primary structural elements for this study are Doubly reinforced, One-way RC slabs with both simple and fixed support end conditions. Three strength classes of RC concrete incorporating available construction materials were investigated; Normal strength (NSC/NSR), Medium strength (MSC/MSR), and High strength (HSC/HSR). Nine bilinear shock loading profiles were considered by pairing various levels of peak pressures and durations to expose the investigated RC slabs to damage levels varying from superficial to severe damage. RCBlast program, a SDOF tool, was utilized to predict blast responses of the investigated RC slabs by modelling their geometries, boundary conditions, rebar arrangements, materials properties, strain-rate effects, damage extents and blast loading profiles. The following provides description of the various aspects of the current investigation.

Investigated RC Slab

A slab configuration was considered that has similar geometry (i.e. span, width, thickness) to those previously tested RC specimens but has both top and bottom flexural reinforcements. Figure 13 shows typical geometric and rebar arrangements for the investigated RC slabs.

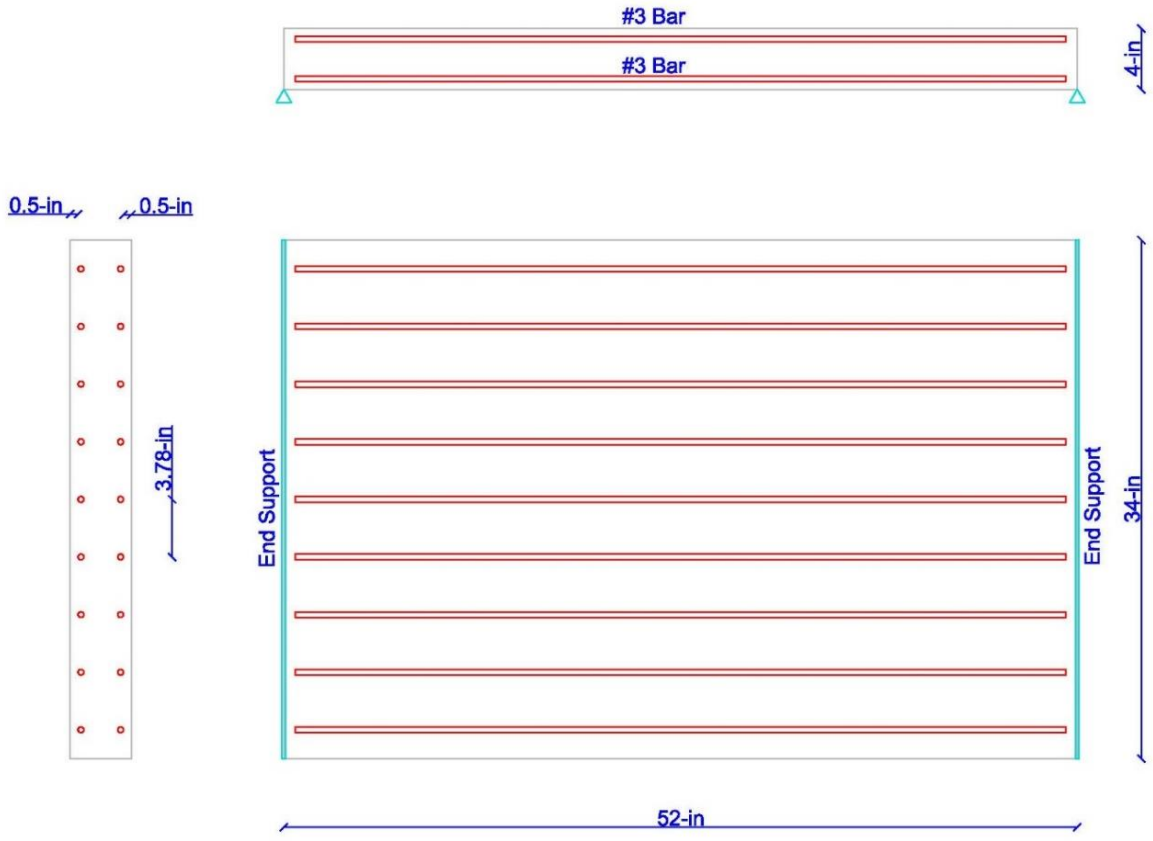

Figure 13 Investigated One-Way RC Slab

Study Cases

To account for most of the practical design cases that involve various material strengths (Normal, Medium, High), boundary conditions (Simple and Fixed End Supports), and blast loading intensities (Low, Medium, High), a total of 54 analysis cases were considered. Table 5 provides a list of the analysis cases with corresponding parameters.

Table 5: Summary of Study Cases

Analysis Case	Conc. Type	Rebar Type	BCs	Blast Load		Analysis Case	Conc. Type	Rebar Type	BCs	Blast Load
Case-1	NSC	NSR	S-S	BL1		Case-28	NSC	NSR	F-F	BL1
Case-2	MSC	MSR	S-S	BL1		Case-29	MSC	MSR	F-F	BL1
Case-3	HSC	HSR	S-S	BL1		Case-30	HSC	HSR	F-F	BL1
Case-4	NSC	NSR	S-S	BL2		Case-31	NSC	NSR	F-F	BL2
Case-5	MSC	MSR	S-S	BL2		Case-32	MSC	MSR	F-F	BL2
Case-6	HSC	HSR	S-S	BL2		Case-33	HSC	HSR	F-F	BL2
Case-7	NSC	NSR	S-S	BL3		Case-34	NSC	NSR	F-F	BL3
Case-8	MSC	MSR	S-S	BL3		Case-35	MSC	MSR	F-F	BL3
Case-9	HSC	HSR	S-S	BL3		Case-36	HSC	HSR	F-F	BL3
Case-10	NSC	NSR	S-S	BL4		Case-37	NSC	NSR	F-F	BL4
Case-11	MSC	MSR	S-S	BL4		Case-38	MSC	MSR	F-F	BL4
Case-12	HSC	HSR	S-S	BL4		Case-39	HSC	HSR	F-F	BL4
Case-13	NSC	NSR	S-S	BL5		Case-40	NSC	NSR	F-F	BL5
Case-14	MSC	MSR	S-S	BL5		Case-41	MSC	MSR	F-F	BL5
Case-15	HSC	HSR	S-S	BL5		Case-42	HSC	HSR	F-F	BL5
Case-16	NSC	NSR	S-S	BL6		Case-43	NSC	NSR	F-F	BL6
Case-17	MSC	MSR	S-S	BL6		Case-44	MSC	MSR	F-F	BL6
Case-18	HSC	HSR	S-S	BL6		Case-45	HSC	HSR	F-F	BL6
Case-19	NSC	NSR	S-S	BL7		Case-46	NSC	NSR	F-F	BL7
Case-20	MSC	MSR	S-S	BL7		Case-47	MSC	MSR	F-F	BL7
Case-21	HSC	HSR	S-S	BL7		Case-48	HSC	HSR	F-F	BL7
Case-22	NSC	NSR	S-S	BL8		Case-49	NSC	NSR	F-F	BL8
Case-23	MSC	MSR	S-S	BL8		Case-50	MSC	MSR	F-F	BL8
Case-24	HSC	HSR	S-S	BL8		Case-51	HSC	HSR	F-F	BL8
Case-25	NSC	NSR	S-S	BL9		Case-52	NSC	NSR	F-F	BL9
Case-26	MSC	MSR	S-S	BL9		Case-53	MSC	MSR	F-F	BL9
Case-27	HSC	HSR	S-S	BL9		Case-54	HSC	HSR	F-F	BL9

Concrete Properties

To investigate the influence that concrete strength may have on the blast response of RC slabs, three classes of concrete were considered: Normal Strength Concrete (NSC) with f_c' = 5,000 psi, Medium Strength Concrete (MSC) with f_c' = 10,000 psi and High Strength Concrete (HSC) with f_c' = 15,000 psi.

Table 6 provides concrete physical and mechanical properties as assumed or obtained from CEB-FIP 2010 [1] and fib Bulletin 42 [2]. Figure 14 shows compressive stress-strain curves constructed using provisions of CEB-FIP 2010 for all concrete classes.

Table 6: Physical and Mechanical Properties of Concrete of Various Strengths

Property	**Symbol**	**Unit**	**NSC 5,000 psi**	**MSC 10,000 psi**	**HSC 15,000 psi**
Specific Weight	γ_c	pcf	145	145	145
Cyl. Compressive Strength	$f_{c'}$	psi	5,000	10,000	15,000
Cyl. Tensile Strength	f_t	psi	440	635	750
Elastic Modulus (Mean)	E_c	psi	3,825,000	4,819,000	5,516,500
Poisson's Ratio	ν_c		0.197	0.214	0.232
Limit Compressive Strain	$\varepsilon_{c\text{-}max}$		0.0035	0.0032	0.0030
Maximum Aggregate Size	d_{agg}	in	3/8	3/8	3/8
Strength Increase Factor	SIF_c		1.00	1.00	1.00
Dynamic Increase Factor	DIF_c		1.344	1.170	1.113

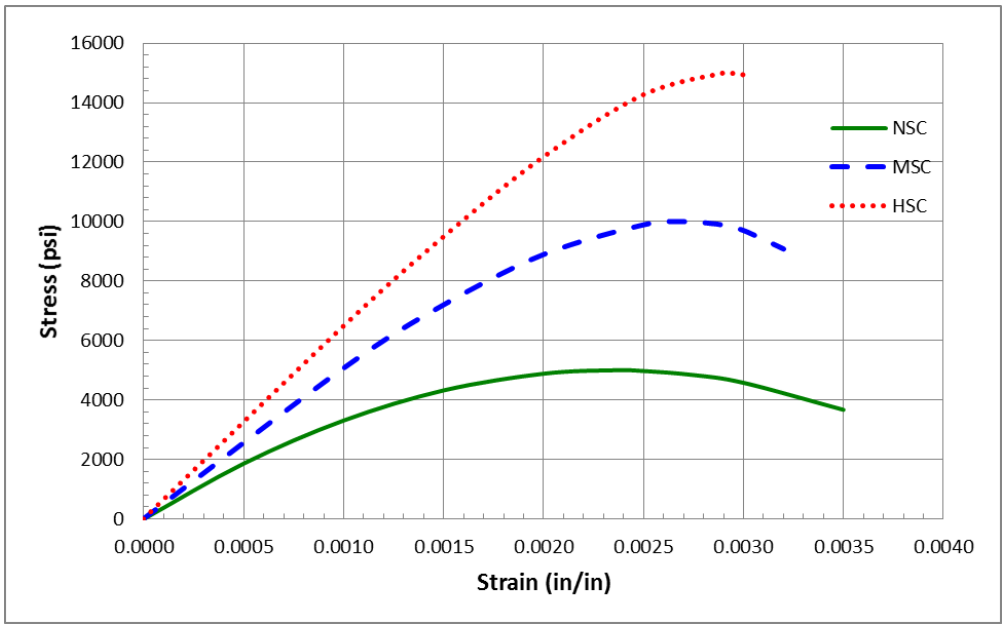

Figure 14- Static Engineering Stress Strain Curves of Concrete of Various Strengths

Steel Rebar Properties

To evaluate the influence of steel rebar strength on blast response of RC slabs, three classes of steel rebar were considered. ASTM A615-GR-60 ksi steel typically used for reinforcing bars of concrete was selected to represent Normal Strength Rebar (NSR). ASTM A615-GR-75 ksi steel, a mid-range reinforcing steel was selected to represent Medium Strength Rebar (MSR). A1035-Gr-100 ksi, a newly developed specialty reinforcing steel was selected to represent High Strength Rebar (HSR).

Table 7 shows physical and mechanical properties for various steel strengths including DIFs as recommended by Malvar [6]. Figures 15, 16 show static engineering and dynamic true stress-strain curves respectively for rebar steels as implemented in the current study.

Table 7: Physical and Mechanical Properties of Steel Rebar of Various Strengths

Property	**Symbol**	**Unit**	**NSR A615 Gr-60**	**MSR A615 Gr-75**	**HSR A1035 Gr-100**
Specific Weight	γ_s	pcf	490	490	490
Initial Yield Strength	F_y	psi	60,000	75,000	100,000
Strain Hardening Strength	F_{sh}	psi	63,000	79,000	105,000
Ultimate (Tensile) Strength	F_u	psi	92,000	105,000	165,000
Elastic Modulus (Initial)	E_s	psi	29,000,000	29,000,000	29,000,000
Poisson's Ratio	ν_s		0.300	0.300	0.300
Limit Tensile Strain	$\varepsilon_{t\text{-}max}$		0.145	0.135	0.110
Strength Increase Factor	SIF_s		1.20	1.100	1.00
Dynamic Increase Factor	DIF_s		1.260	1.185	1.068

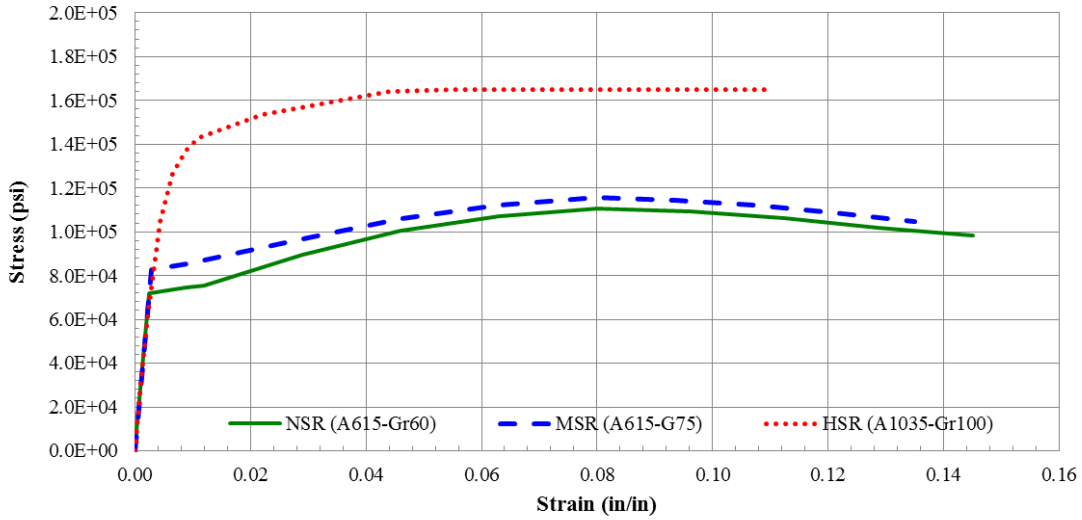

Figure 15- Static Engineering Stress Strain Curves of Steel Rebar of Various Strengths

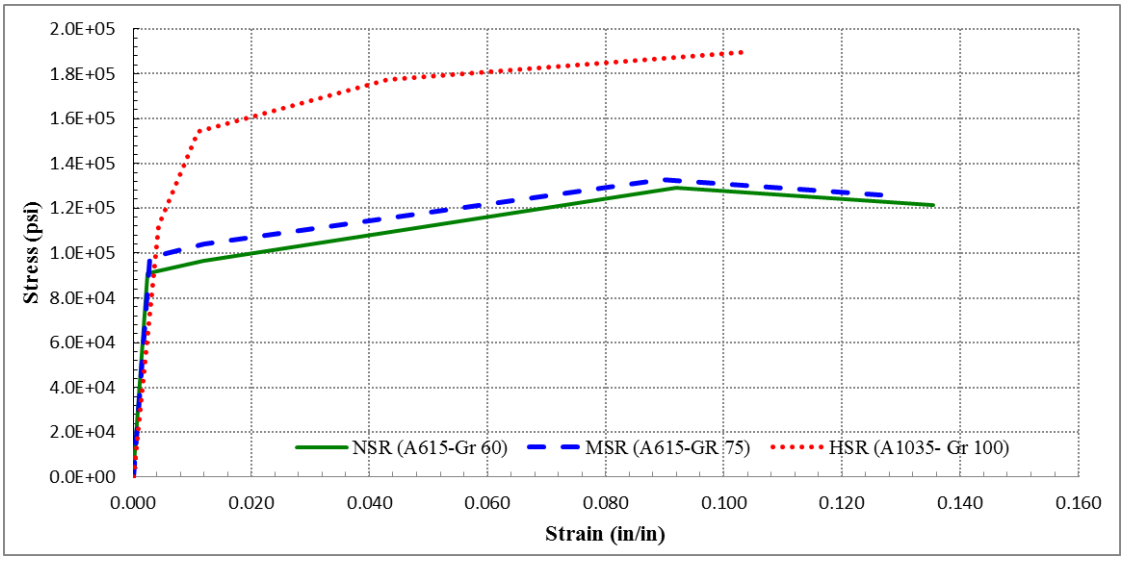

Figure 16- Dynamic True Stress Strain Curves of Steel Rebar of Various Strengths

Blast Loading

To encompass the practical range of blast loading that the investigated RC slabs could be designed for, the study considered nine bilinear shock loading profiles varying in load intensity and duration. The bilinear pulse shape was selected as a good approximation to either the exponential decay shock pressure signature corresponding to unconfined high explosive detonation or to the combined shock and gas pressure phases of partially confined detonations. Three pressure intensities were selected based on the blast resistances of considered RC slabs to cover load intensity to resistance (P/r_u) ratio that varies approximately from 0.50 to 2.50.

Considered pressure intensities were relatively classified as: Low Pressure (LP) of 30 psi, Medium Pressure (MP) of 45 psi, and High Pressure (HP) of 60 psi. Three total durations were selected based on the fundamental periods of considered RC slabs to cover load duration to fundamental period (T/T_N) ratio that varies approximately from 0.50 to 3.50. Considered durations include: Short Duration (SD) of 10 msec, Medium Duration (MD) of 20 msec, and Long Duration (LD) of 40 msec. Blast Loads BL1 through BL9 were compiled by pairing various pressure intensities with various durations. Figure 17 shows the bilinear profile of a typical blast load curve. Table 8 provides relevant blast load information including curve points (t_i, P_i) identifying bilinear profile of each load curve, total blast impulse (I_{tot}), as a measure of blast energy, and equivalent triangular pulse duration (T).

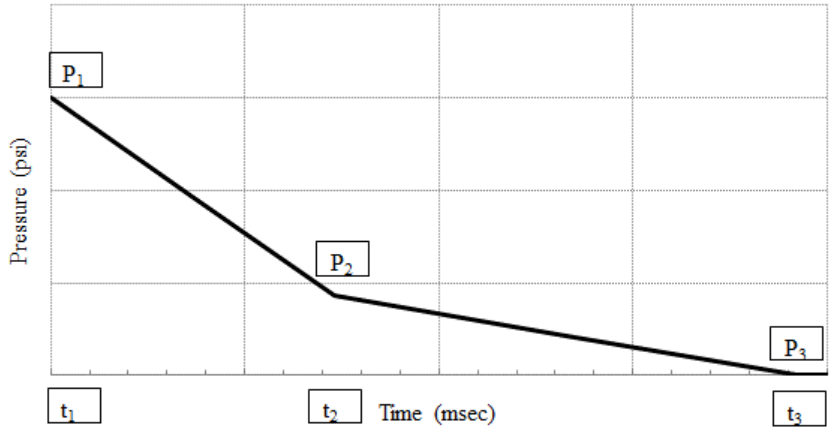

Figure 17- Typical Bilinear Blast Load Time History

Table 8: Bilinear Blast Load Curves Parameters

Blast Load ID	Class	t_1 (ms)	P_1 (psi)	t_2 (ms)	P_2 (psi)	t_3 (ms)	P_3 (psi)	I_{tot} (psi-ms)	T (ms)
BL1	LP/SD	0.00	30.0	6.72	8.72	18.00	0.0	179.0	9.48
BL2	LP/MD	0.00	30.0	14.64	8.63	38.50	0.0	386.0	20.55
BL3	LP/LD	0.00	30.0	28.08	8.71	75.00	0.0	748.0	39.56
BL4	MP/SD	0.00	45.0	6.72	13.08	18.00	0.0	269.0	9.48
BL5	MP/MD	0.00	45.0	14.64	12.99	38.67	0.0	580.0	20.55
BL6	MP/LD	0.00	45.0	28.08	13.06	75.00	0.0	1122.0	39.56
BL7	HP/SD	0.00	60.0	6.72	17.44	18.00	0.0	359.0	9.48
BL8	HP/MD	0.00	60.0	14.64	17.25	38.50	0.0	771.0	20.55
BL9	HP/LD	0.00	60.0	28.08	17.42	75.00	0.0	1496.0	39.56

Component Response Limits and Damage Levels

The primary objective of blast-resistant design of a facility is to provide adequate safety to its occupants and sensitive contents. This is typically communicated to the design professional though an identified Level Of Protection (LOP). To achieve the protection objectives, the blast-resistant design needs to secure adequate strength and ductile detailing to control the blast-induced damage that may be experienced by a component when exposed to the design-level blast event. Figure 18 shows typical damage levels as represented by a component Pressure-Impulse (P-I) capacity as depicted in (PDC 2006) [10]. Acceptable structural damage corresponding to various LOP are typically correlated with maximum structural response limits. Table 9 shows an example of such correlation for RC slabs as obtained from PDC 2006.

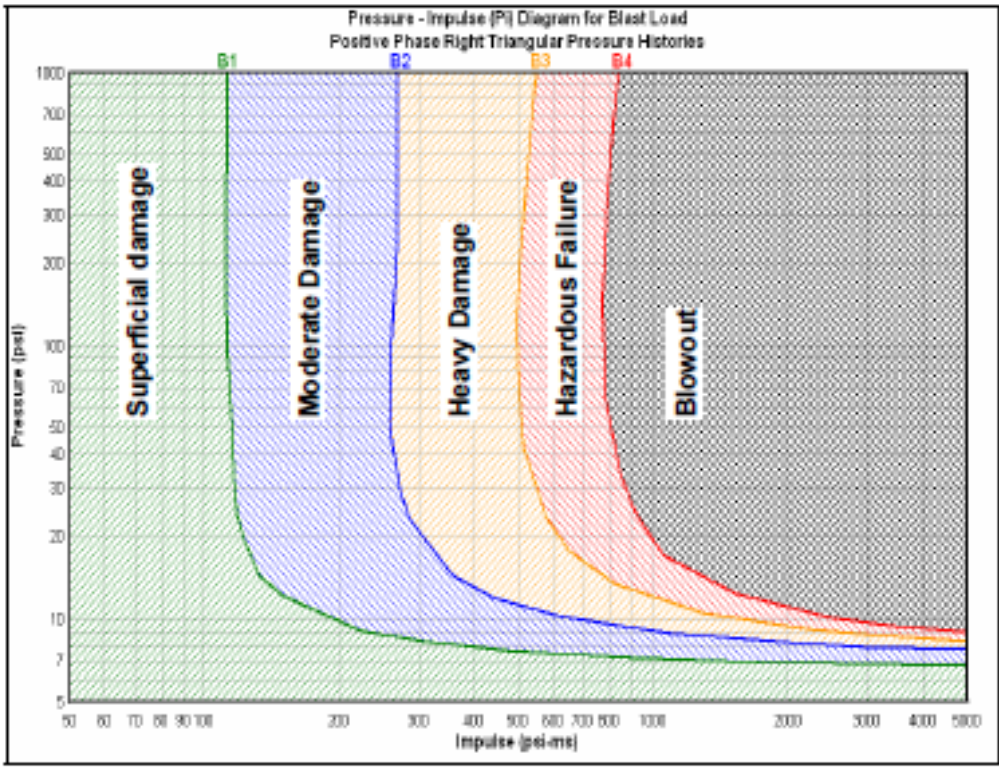

Figure 18- Pressure Impulse Diagram Showing Component Damage Levels (PDC 2006) [10]

Table 9: Response Limits for Various Damage Levels of RC Slabs* (PDC 2006) [10]

Damage Level B1		**Damage Level B2**		**Damage Level B3**		**Damage Level B4**		**Damage Level B5**	
Superficial Damage		Moderate Damage		Heavy Damage		Hazardous Failure		Blowout	
μ	θ	μ	θ	μ	θ	μ	θ	μ	θ
1.0	-	-	2 °	-	5 °	-	10 °	-	> 10 °

* Flexural Response with No Shear Reinforcement and without Tension Membrane

DISCUSSION OF RESULTS

This section of the paper provides comprehensive tabulated and graphical representations of the study results combined with brief discussion of how the computed structural responses correlate to the properties of the blast-loaded RC slabs with emphasis on material strength.

Computed SDOF Properties

Tables 10, 11 show the primary SDOF parameters and Figures 19, 20 show the resistance-displacement curves all computed by RCBlast for reinforced concrete slabs of various strengths (NS, MS, HS) with Simple and Fixed supports respectively. The primary observation is that despite the considerable variation in both concrete and rebar strengths (i.e. 300% for f'_c and 67% for f_y), the variations in the computed primary dynamic properties (K_E, r_u, T_N) of the investigated slabs were one order of magnitude lower than the strength ratio level and they were in the order of 13%, 25%, and 7% respectively.

That can be attributed to the fact that both the Strength Increase Factors (SIF) and the Dynamic Increase Factors (DIF) for concrete and rebar steel decrease as the material strength gets higher. In addition, flexural strength of a RC slab and hence its blast resistance is predominantly controlled by its rebar properties. In addition the initial stiffness of a RC slab is primarily influenced by its concrete modulus which is a function of the square root of its compressive strength ($\sqrt{f'_c}$) and tend to have a lower proportionality to ($\sqrt{f'_c}$) as the concrete strength increases. Having the same mass and slightly varying stiffness resulted in having RC slabs with close fundamental periods of vibration.

It is worth noting the close similarities between Normal strength (NSC/NSR) and the Medium strength (MSC/MSR) concrete properties and their resistance-displacement profiles (See Figure 19) which indicate the limited blast-resistance benefits of specifying Medium strength class over the Normal strength class especially when construction costs are taken into consideration.

Table 10: SDOF Properties of Simple Supports RC Slabs of Various Strengths (RCBlast)

Property	**Symbol**	**Unit**	**NSC/NSR Slab**	**MSC/MSR Slab**	**HSC/HSR Slab**
Mass	M	psi.ms^2/in	869	869	869
Load-Mass Factors	K_{LM}		0.78,0.78, 0.66	0.78,0.78, 0.66	0.78,0.78, 0.66
Stiffness (Initial)	K_E	psi/in	49.58	45.83	43.12
Plastic Hinge Length	L_p	in	7.48	8.46	9.84
Flex. Resistance (Ultimate)	r_u	psi	29.05	30.64	44.68
Yield Displacement (Equiv.)	X_E	in	0.305	0.366	0.438
Fundamental Period	T_N	msec	18.66	19.41	20.02

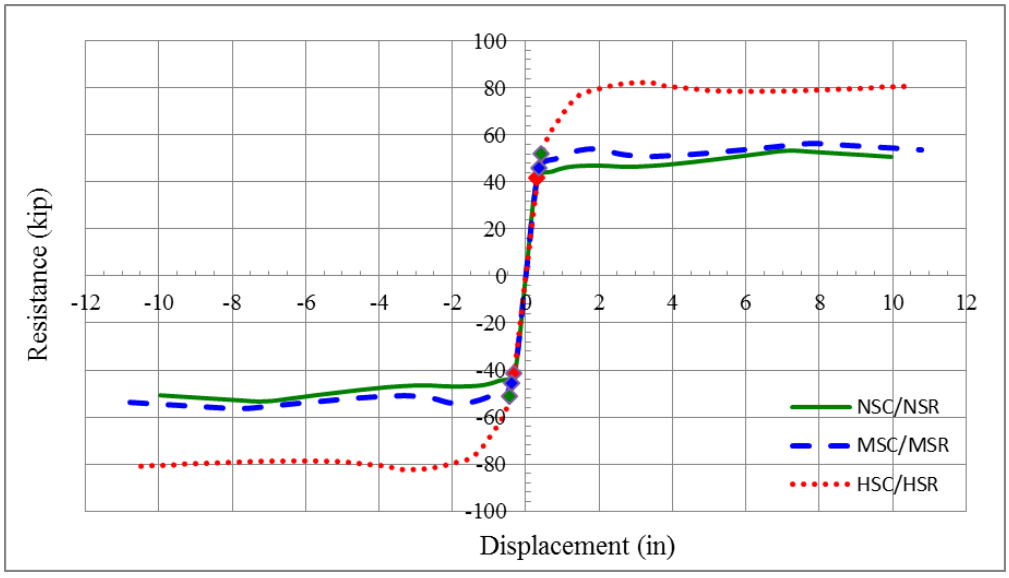

Figure 19- Resistance-Displacement Curves of (S-S) RC Slabs of Various Strengths

Table 11: SDOF Properties of Fixed Supports RC Slabs of Various Strengths (RCBlast)

Property	**Symbol**	**Unit**	**NSC/NSR Slab**	**MSC/MSR Slab**	**HSC/HSR Slab**
Mass	M	psi.ms^2/in	869	869	869
Load-Mass Factors	K_{LM}		0.77,0.78, 0.66	0.77,0.78, 0.66	0.77,0.78, 0.66
Stiffness (Initial)	K_E	psi/in	112.53	116.08	129.2
Plastic Hinge Length	L_p	in	7.48	8.46	9.84
Flex. Resistance (Ultimate)	r_u	psi	58.04	61.24	89.24
Yield Displacement (Equiv.)	X_E	in	0.230	0.260	0.283
Fundamental Period	T_N	msec	12.31	12.12	11.49

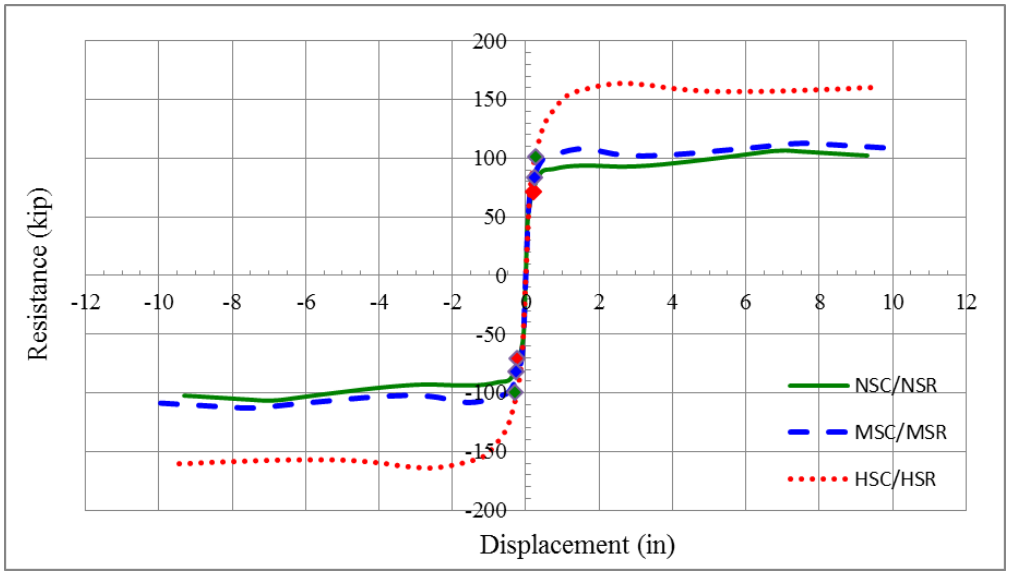

Figure 20- Resistance-Displacement Curves of (F-F) RC Slabs of Various Strengths

Computed Maximum Structural Responses to Blast Loading

Table 12 provides a summary of blast response results for all 54 cases as computed by RCBlast program. The primary RC response results include: T/T_N (Load Duration-to-Fundamental Period Ratio), P/r_u (Load Intensity-to-Resistance Ratio), T_y (Time for 1st yield), T_{max} (Time for Maximum mid-displacement), X_{max} (Maximum mid-displacement), θ_{max} (Maximum slab-end rotation), X_{res} (Residual mid-displacement), and Damage Index (as per PDC 2006).

Table 12: Blast Response Results for Investigated Cases (RCBlast)

Analysis Case	**RC Class**	**T/T_N**	**P/r_u**	**T_y (msec)**	**T_{max} (msec)**	**X_{max} (in)**	**θ_{max} (deg)**	**X_{res} (in)**	**PDC Damage Index**
Case-1	NS	0.508	1.033	4.20	8.80	0.516	1.14	0.102	B2
Case-2	MS	0.488	0.979	5.20	8.60	0.516	1.14	0.063	B2
Case-3	HS	0.474	0.671	6.00	8.30	0.520	1.15	0.024	B2
Case-4	NS	1.101	1.033	3.90	13.00	0.941	2.07	0.382	B3
Case-5	MS	1.059	0.979	4.80	12.00	0.866	1.91	0.260	B2
Case-6	HS	1.026	0.671	5.30	10.50	0.772	1.70	0.118	B2
Case-7	NS	2.120	1.033	3.90	18.40	1.472	3.24	1.031	B3
Case-8	MS	2.038	0.979	4.60	15.80	1.224	2.70	0.701	B3
Case-9	HS	1.976	0.671	5.20	12.00	0.937	2.06	0.272	B3
Case-10	NS	0.508	1.549	3.20	11.40	1.031	2.27	0.362	B3
Case-11	MS	0.488	1.469	3.90	10.60	0.965	2.12	0.268	B3
Case-12	HS	0.474	1.007	4.40	9.30	0.866	1.91	0.134	B2
Case-13	NS	1.101	1.549	3.10	19.00	2.512	5.52	1.878	B4
Case-14	MS	1.059	1.469	3.70	16.60	2.091	4.60	1.315	B3
Case-15	HS	1.026	1.007	4.10	12.50	1.453	3.20	0.421	B3
Case-16	NS	2.120	1.549	3.10	29.20	5.043	10.98	4.488	B5
Case-17	MS	2.038	1.469	3.70	26.90	4.059	8.87	3.465	B4
Case-18	HS	1.976	1.007	4.00	15.80	1.929	4.24	1.130	B3
Case-19	NS	0.508	2.065	2.70	14.00	1.807	3.98	0.902	B3
Case-20	MS	0.488	1.958	3.30	12.80	1.614	3.55	0.650	B3
Case-21	HS	0.474	1.343	3.60	10.30	1.283	2.83	0.276	B3
Case-22	NS	1.101	2.065	2.70	23.90	4.724	10.30	4.071	B5
Case-23	MS	1.059	1.958	3.10	22.10	4.059	8.87	3.402	B4
Case-24	HS	1.026	1.343	3.50	14.70	2.362	5.19	1.209	B4
Case-25	NS	2.120	2.065	2.70	32.30	7.760	16.62	7.217	B5
Case-26	MS	2.038	1.958	3.10	31.00	6.898	14.86	6.303	B5
Case-27	HS	1.976	1.343	3.50	20.30	3.346	7.33	2.583	B4
Case-28	NS	0.770	0.517	N/A	4.50	0.142	0.31	0.000	B0
Case-29	MS	0.782	0.490	N/A	4.20	0.138	0.30	0.000	B0
Case-30	HS	0.825	0.336	N/A	4.10	0.142	0.31	0.000	B0
Case-31	NS	1.669	0.517	N/A	5.40	0.181	0.40	0.000	B0
Case-32	MS	1.696	0.490	N/A	4.80	0.165	0.36	0.000	B0
Case-33	HS	1.789	0.336	N/A	4.50	0.165	0.36	0.000	B0
Case-34	NS	3.214	0.517	N/A	6.00	0.209	0.46	0.000	B0

Case-35	MS	3.264	0.490	N/A	5.10	0.181	0.40	0.000	B0
Case-36	HS	3.443	0.336	N/A	4.70	0.177	0.39	0.000	B0
Case-37	NS	0.770	0.775	3.80	5.70	0.295	0.65	0.020	B1
Case-38	MS	0.782	0.735	4.90	5.20	0.260	0.57	0.000	B0
Case-39	HS	0.825	0.504	N/A	4.80	0.240	0.53	0.000	B0
Case-40	NS	1.669	0.775	3.40	7.40	0.437	0.96	0.087	B1
Case-41	MS	1.696	0.735	3.90	6.60	0.366	0.81	0.039	B1
Case-42	HS	1.789	0.504	4.40	5.60	0.307	0.68	0.008	B1
Case-43	NS	3.214	0.775	3.30	8.90	0.539	1.19	0.209	B2
Case-44	MS	3.264	0.735	3.70	7.40	0.429	0.95	0.094	B1
Case-45	HS	3.443	0.504	4.20	6.00	0.339	0.75	0.024	B1
Case-46	NS	0.770	1.034	2.80	6.80	0.520	1.15	0.114	B2
Case-47	MS	0.782	0.980	3.10	6.20	0.449	0.99	0.067	B1
Case-48	HS	0.825	0.672	3.40	5.40	0.378	0.83	0.024	B1
Case-49	NS	1.669	1.034	2.70	10.30	0.945	2.08	0.500	B3
Case-50	MS	1.696	0.980	3.00	8.80	0.728	1.60	0.291	B2
Case-51	HS	1.789	0.672	3.20	6.50	0.504	1.11	0.087	B2
Case-52	NS	3.214	1.034	2.27	14.30	1.382	3.04	1.028	B3
Case-53	MS	3.264	0.980	2.90	11.20	0.949	2.09	0.587	B3
Case-54	HS	3.443	0.672	3.10	7.20	0.563	1.24	0.177	B2

Figures 21 through 29 depict maximum mid-span displacement histories of simply-supported RC slabs (Cases 1 through 27) of various strength classes (NSC/NSR, MSC/MSR, HSC/HSR) when subjected to various blast loading (Bl through BL9) as computed by RCBlast program.

For illustration purposes, Figures 30 through 32 depict maximum mid-span displacement histories of Fixed-supports RC slabs (Cases 52 through 54) of various strength classes (NSC/NSR, MSC/MSR, HSC/HSR) when subjected to High-Pressure blast loading (i.e. BL7, BL8, BL9).

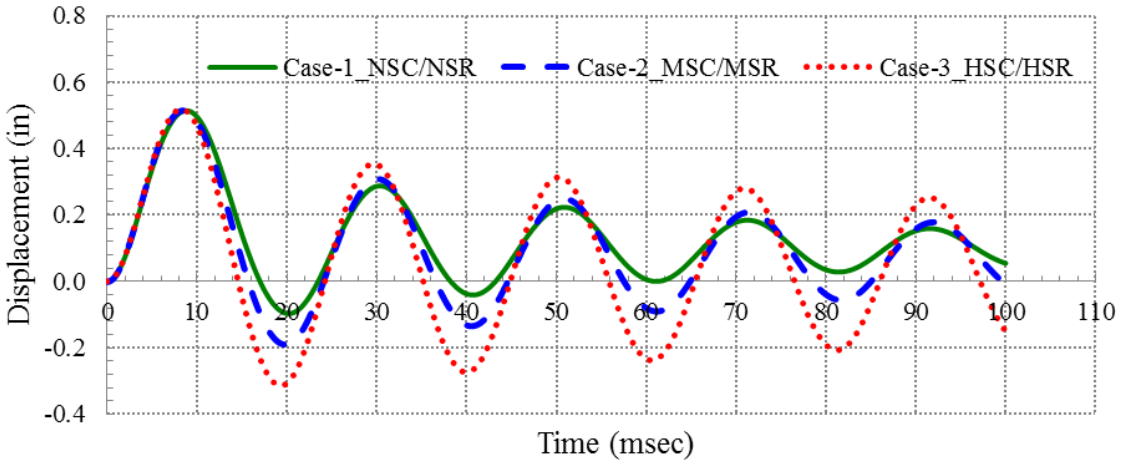

Figure 21- Maximum Displacement Responses of SS RC Slabs to Blast BL1

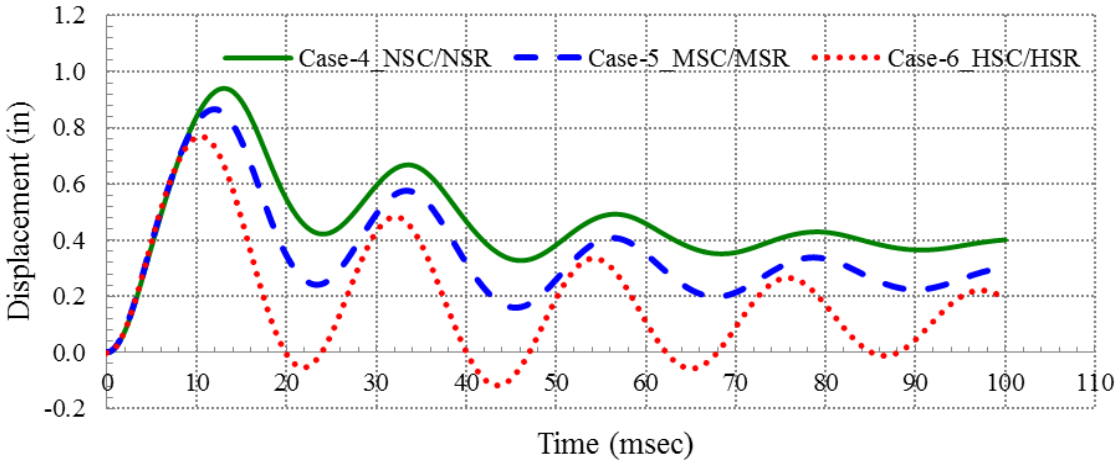

Figure 22- Maximum Displacement Responses of SS RC Slabs to Blast BL2

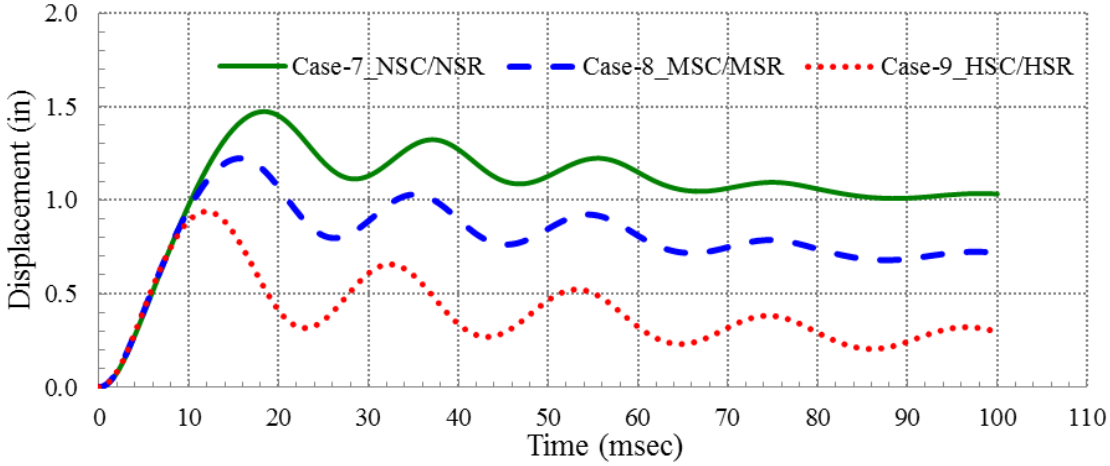

Figure 23- Maximum Displacement Responses of SS RC Slabs to Blast BL3

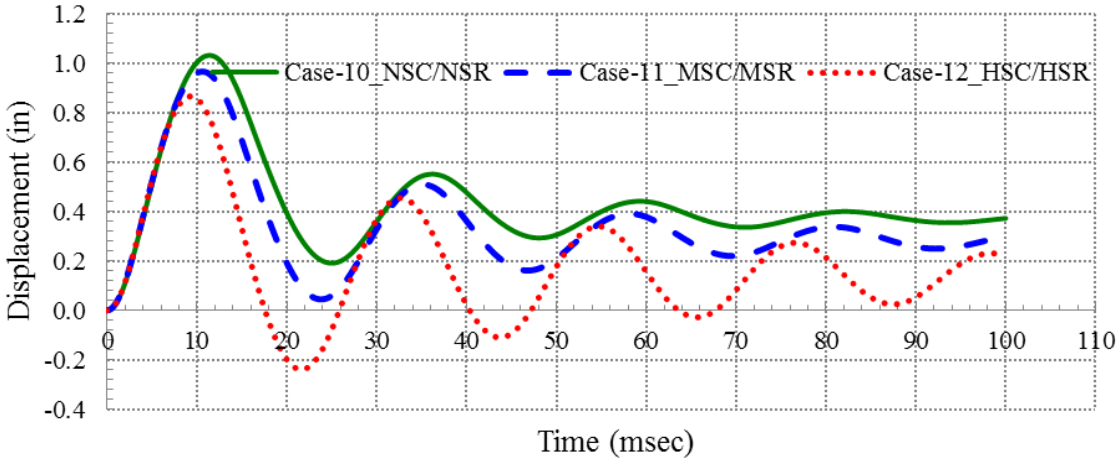

Figure 24- Maximum Displacement Responses of SS RC Slabs to Blast BL4

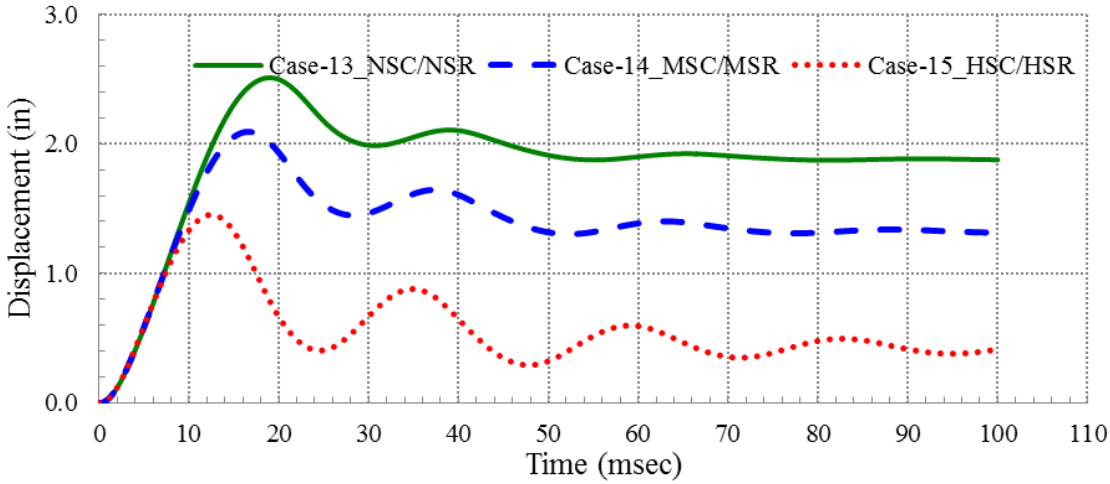

Figure 25- Maximum Displacement Responses of SS RC Slabs to Blast BL5

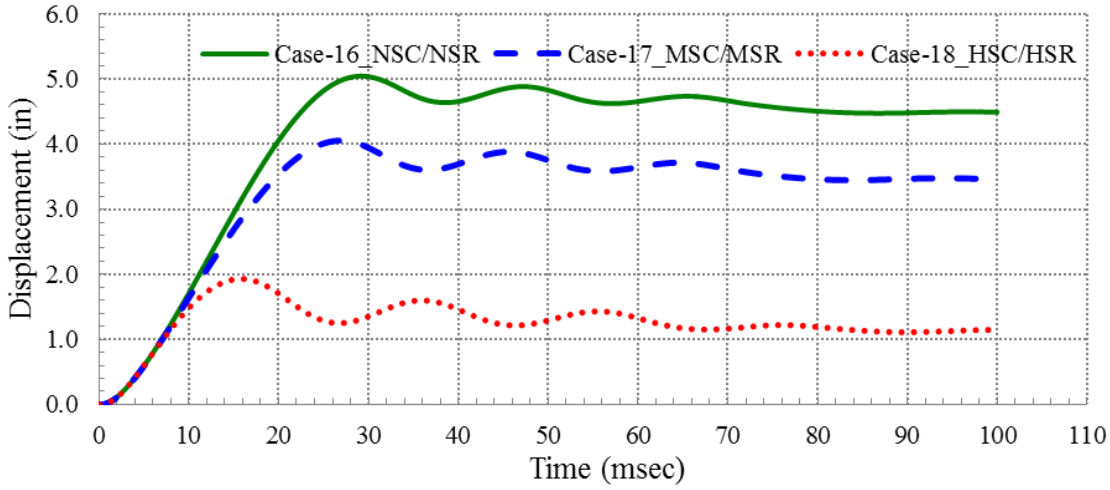

Figure 26- Maximum Displacement Responses of SS RC Slabs to Blast BL6

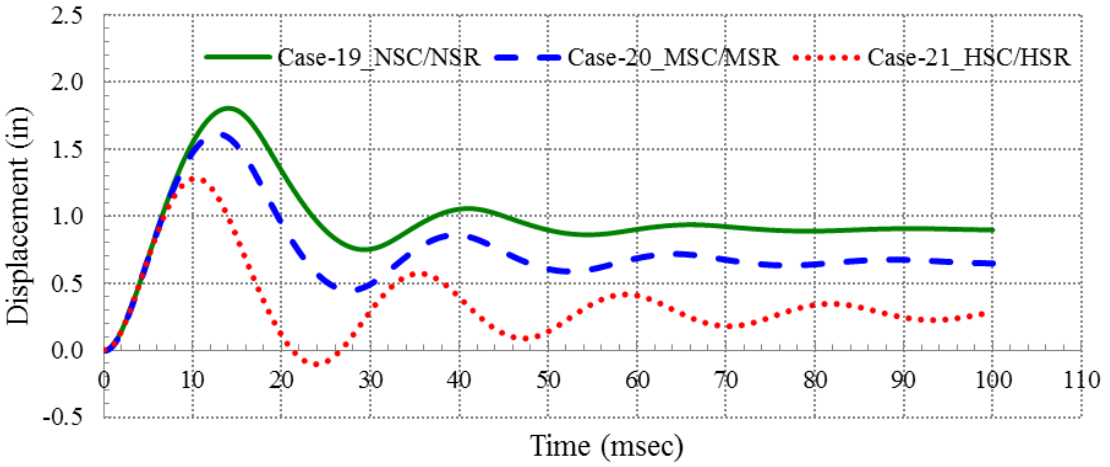

Figure 27- Maximum Displacement Responses of SS RC Slabs to Blast BL7

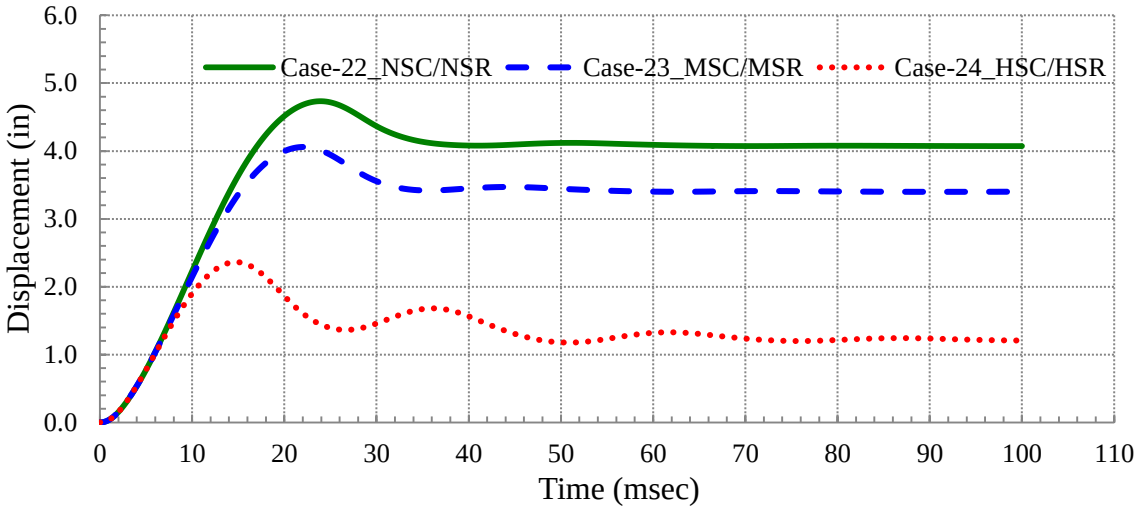

Figure 28- Maximum Displacement Responses of SS RC Slabs to Blast BL8

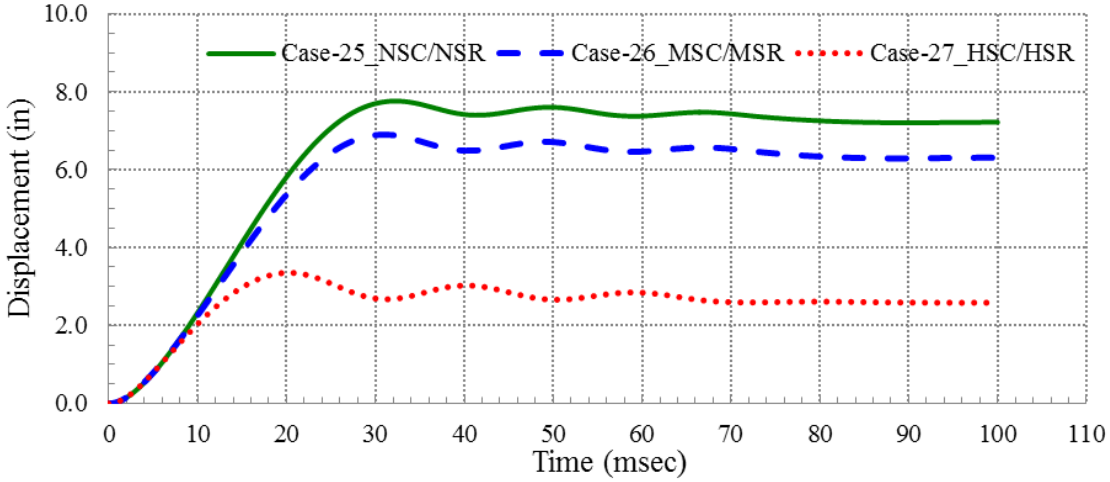

Figure 29- Maximum Displacement Responses of SS RC Slabs to Blast BL9

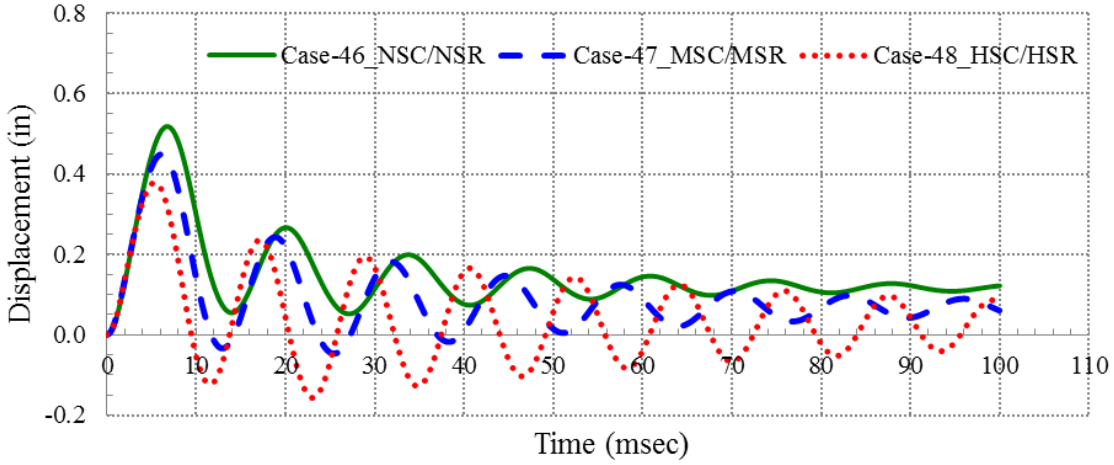

Figure 30- Maximum Displacement Responses of FF RC Slabs to Blast BL7

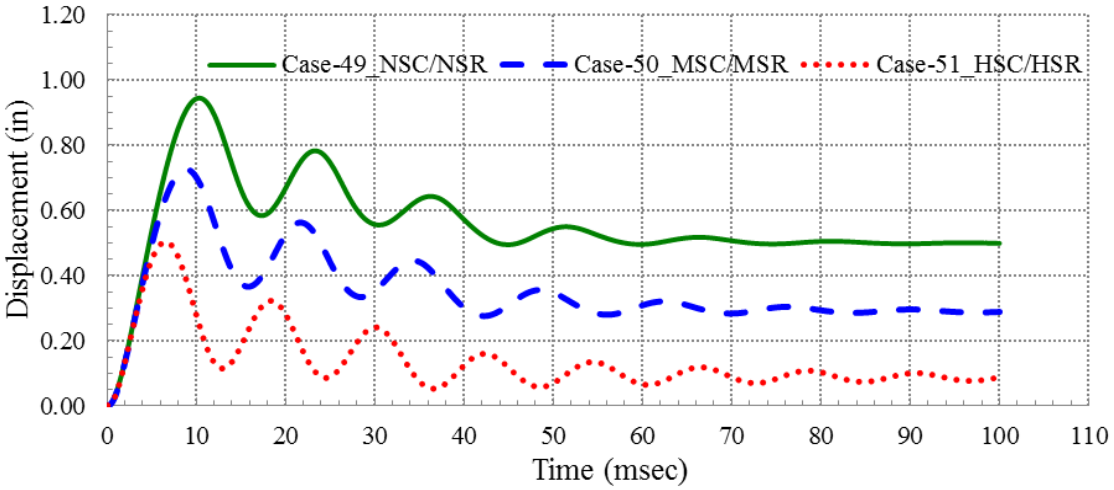

Figure 31- Maximum Displacement Responses of FF RC Slabs to Blast BL8

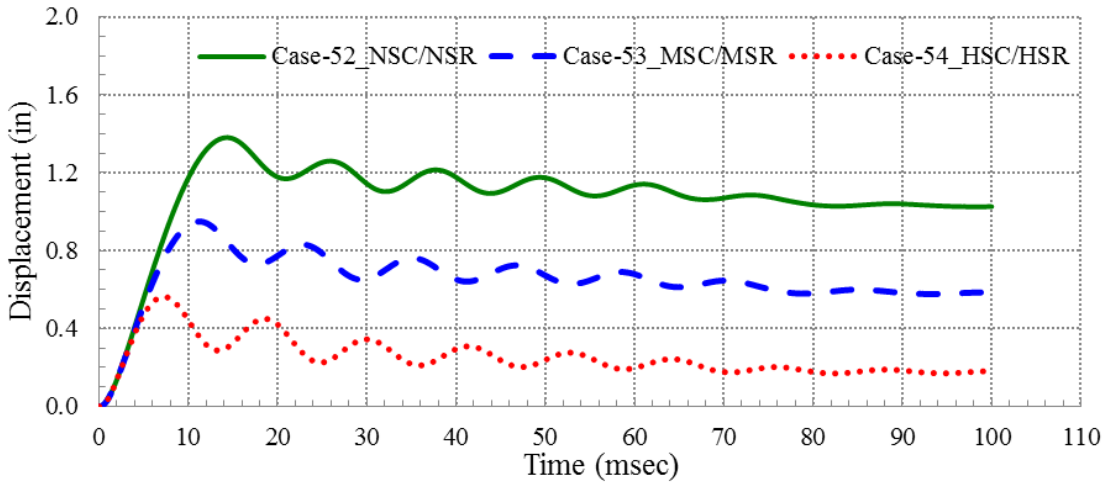

Figure 32- Maximum Displacement Responses of FF RC Slabs to Blast BL9

CONCLUSIONS

General

1- When making a decision about using a higher strength class to achieve better blast-resistant performance, it is important to consider that the favorable changes in the primary dynamic properties (i.e. Stiffness, Resistance, and Fundamental Period) are one order of magnitude lower than that of the strength ratio. Therefore, the emphasis should not be on the use of "stronger" concrete materials, rather it should be on the use of "tougher" concrete materials and proper detailing that can effectively sustain the blast energy in a ductile manner with limited structural response and damage extents.

2- As expected the level of blast-induced damage experienced by RC slabs increases as the blast loading intensity (i.e. peak pressure) and/or energy (i.e. total impulse) increases. The predicted damage level- expressed through maximum end rotation, maximum and residual

displacements- showed dependence on the RC strength class that varied according to the blast loading characteristics.

3- The most influential parameters affecting the response of structures to impulsive-like loading are: the Load Duration-to-Fund. Period Ratio (T/T_N) and the Load Intensity-to-Resistance Ratio (P/r_u). Understanding the response dependence on these non-dimensional ratios allows the analyst/ designer to successfully predict the response to blast loads using simplified SDOF approaches. Graphical solution charts of UFC 3-340-02 are considered valuable tools for element sizing at planning level and for verification of final designs with acceptable practical accuracy.

4- The use of higher strength class produces a RC slab with higher flexural resistance, higher equivalent yield displacement, lower initial stiffness, longer plastic hinge length, and lower fundamental period. Typically, the blast response of such a slab will exhibit reduced maximum response (X_{max}), support rotation (θ_{max}) and residual damage (X_{res}) than those for lower strength class. It will also indicate a delayed time for initial yield (T_y) and an earlier time for maximum response (T_{max}).

5- When evaluating construction material alternatives for blast-resistance, it is not sufficient to consider the absolute reduction in structural response and damage resulting from the use of stronger materials as the only selection criterion. It is essential to conduct a cost-benefit analysis to compare the added value (i.e. protection) obtained using a higher strength class to the design/ construction costs incurred. It is also essential to understand the range of cost-effectiveness of various material strengths for different levels of blast load severity (i.e. intensity and energy content).

For Simply Supported RC Slabs

6- Acknowledging the acceptance of heavy damage for most blast-resistant designs (i.e. PDC damage index B3), the use of NSC/NSR proved to be adequate for Low Pressure; LP blast loading within the Load Intensity-to-Resistance Ratio range of ($P/r_u < 2.25$) for any blast duration. As the blast intensity increases (i.e. MP, HP), the feasibility of using normal strength concrete becomes limited to low energy blast loading, with Short Duration; SD within the Load Duration-to-Fundamental Period Ratio range of ($1.0 > T/T_N \geq 0.5$).

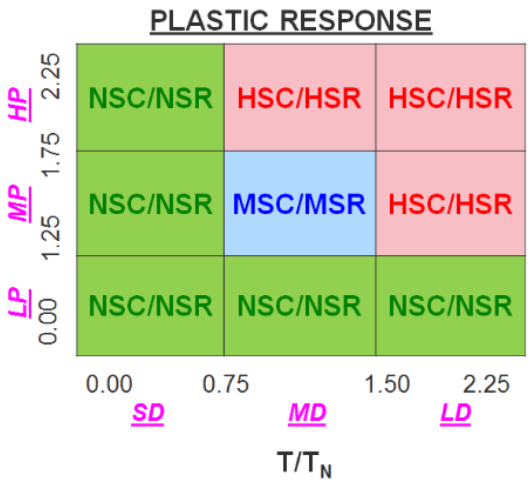

7- The use of MSC/MSR proved to be practical within the narrow range of blast loading that involved Medium Pressure; MP with ($1.5 > P/r_u \geq 1.0$) and Medium Duration; MD with ($1.0 > T/T_N \geq 0.5$). For all other cases, the use of MSC/MSR did not seem to provide noticeable structural performance improvement over the cases using NSC/NSR and despite the relative reduction in blast response, the damage classifications for both RC classes were similar.

8- The use of HSC/HSR proved to be most effective for high energy blast loading with High Pressure; HP with ($1.5 > P/r_u \geq 1.0$) for both Medium Duration; MD with ($1.0 > T/T_N \geq 0.50$) and Long Duration; LD with ($2.0 > T/T_N \geq 1.0$). The use of HSC/HSR for these severe loading conditions reduced the extents of damage and prevented the unacceptable blow out failure of the RC slab.

For Fixed Support RC Slabs

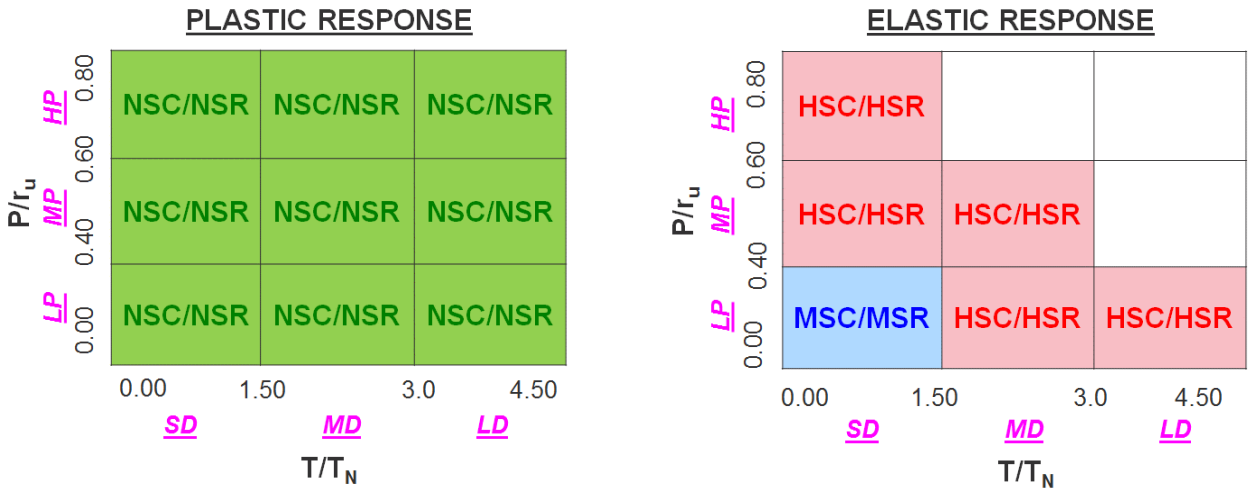

Since a Fixed-Support slab has much higher flexural resistance (r_u), stiffness (K_E), and hence much lower fundamental period (T_N), its structural response and damage due to blast loading is expected to be much less compared to those of a Simple-Support slab. Therefore, the need to use higher strength class of RC diminishes and NSC/NSR would be adequate for most if not for all practical blast-resistant design cases.

9- The use of MSC/MSR or HSC/HSR may be advantageous for design conditions where elastic response is required to accommodate repeated blast load application (e.g. blast containment). This application is more suited for LP blast loading with ($0.5 > P/r_u \geq 0.25$) for any blast duration and for MP blast loading with ($0.75 > P/r_u \geq 0.5$) for SD blast duration with ($1.0 > T/T_N \geq 0.5$).

REFERENCES

[1] International Federation for Structural Concrete (fib), 2010, "CEB-FIP Model Code 2010: First Complete Draft", Lausanne, Switzerland.

[2] International Federation for Structural Concrete (fib), 2008, "Constitutive Modeling of High Strength/ High Performance Concrete: State of the Art Report", Bulletin 42, Lausanne, Switzerland.

[3] Jacques, E., 2014. RCBLAST (Version 0.5.1) Blast Analysis Software

[4] Kewaisy, T.H., 2016, "SDOF and HYDROCODE Simulation of Blast-Loaded Reinforced Concrete Slabs", Technical paper No 7, ACI SP-306, American Concrete Institute, Farmington Hill, MI.

[5] LSDYNA (Version V971 R6.0.0) Software, Livermore Software Technology Corporation (LSTC), Livermore, CA

[6] Malvar, L.J., Crawford, J.E., 1998, "Dynamic Increase Factors for Concrete", Proceedings of the 28th DDESB Seminar, Orlando Florida.

[7].UMKC School of Computing and Engineering, 2013, "Blast Prediction Contest Website http://sce.umkc.edu/blast-prediction-contest/", UMKC.

[8] Unified Facilities Criteria (UFC 03-340-02), 2008, "Structures to resist the effects of accidental explosions", United States of America Department of Defense, Washington, D.C.

[9] U.S. Army Corps of Engineers (USACE)/ Protective Design Center (PDC), 2012. "User's Guide for the Single-Degree-of-Freedom Blast Effects Design Spreadsheets (SBEDS)." PDC-TR 06-02, USACE, Washington, D.C.

[10] U.S. Army Corps of Engineers (USACE)/ Protective Design Center (PDC), 2006, Single-Degree-of-Freedom Structural Response Limits for Antiterrorism Design, PDC-TR 06-08, USACE, Washington, D.C.